Chapter 4 Beamline – main components

B. Carlsen, F. Carvalho, V. De Jesus, J. De La Gama, A. Ebn Rahmoun, R. Froeschl, M. Gourber-Pace, E. Grenier Boley, R. Lopez, R. Mompo, K. Papastergiou, G. Romagnoli, J. Tan, L. Wilhelm

4.1 Magnets

4.1.1 Introduction

The East Area renovation will cover the refurbishment of the East Hall with its beamlines and infrastructures. As defined in Section 2.1, a re-design of the beamlines is included to improve the magnet situation, the radiation situation, and maintainability in general. Thanks to a cycled powering mode of the magnets instead of a steady state one, considerable energy savings will be possible. Therefore, several magnet families have to be re-designed to be in accordance with the purposes of the project.

The new East Area magnet system consists of 12 different designs with a total of 58 magnets among which 15 are bending magnets, 31 are quadrupoles, and 12 are correctors. In the Proton Synchrotron (PS) area (Building 352), the primary area (Building 157), and the line T08 (Building 157), the magnets will be cycled every 2.4 s. This concerns the lines F61, F62, part of F63, and T08. The other lines, T09, T10, and T11, will be cycled with a period of 4.8 s. Cycling the magnets is an important constraint for the construction of the magnetic parts (yokes). In addition, the coils have to be adapted to match the power supply specifications. The magnets have to be laminated to avoid eddy currents and large delays between the magnetic field and the current application. All laminated magnets currently used and needed in the new in the East Area layout will be refurbished, this concerns four families (or 22 units). The new magnets will be manufactured by industry according to CERN's design.

Another constraint is the magnet overall size limitations. As the layout was fixed at the beginning of the project, all new large magnet designs had to have the same length and width as the present ones. This complicates the designs, as laminated yokes need a larger mechanical structure around the yoke to maintain the laminations. The total lengths and widths have been discussed with the integration team and after few iterations a solution was found and the final designs approved.

4.1.2 Bending magnets

Seven C-shaped bending magnets and eight H-shaped bending magnets will be installed in the East Area beamlines. The C-shaped ones are the refurbished MCB bending magnets [1] and the H-shaped will be two new families with different overall lengths from the existing ones but with the same cross-section, the M100 L [2] and M200 L [3]. In Fig. 4-1 it is possible to see the location of these magnets in the East Area.

Fig. 4-1: Bending magnet EEA layout.

4.1.2.1 MCB bending magnets

This type of magnet is being repurposed from old magnets back from the 1970s (see Fig. 4-2). They are part of the bending magnet families made for the Intersecting Storage Ring (ISR) beam transfer system [4]. They are widely used at CERN, in the Experimental Areas, Super Proton Synchrotron (SPS) North Area (NA), and in T10 transfer line. Fourteen units are being used and seven spares are available. The range of integrated field required for the Experimental Areas is from 2.05 to 4.4 Tm, the maximum achievable.

Three of the existing MCB need to be modified before their installation due to the limited power converter voltage; the maximum cycled integrated field achievable with one converter in a 2.4 s period is 3.2 Tm. The large inductance requires the upper and lower coils to be powered separately by two converters. With these different specifications, in addition of the seven units, one spare of each type (four magnets with a single converter and three magnets with two converters) will be prepared, see Table 4-1.

Table 4-1: MCB bending magnet characteristics.

Number of magnets	**4 + 1**	**3 + 1**	
CERN code	PXMBXHDCWP		
Electrical circuits	1		2
Short name	MCB / HB2		
Aperture [mm]	80		
Iron length [mm]	2 500		
Total length [mm]	3 120		
Total width [mm]	1 246		
Total height [mm]	1 250		
Weight [kg]	20 500		
Nominal current [A]	880		
Resistance [mΩ]	165		2 × 82.5
Inductance [mH]	640		2 × 320
Power at nominal current [kW]	128		2 × 64
Delta P nominal [bar]	15		
Nominal cooling flow [l/min]	56		
Total number of turns	204		2 × 102
Nominal field [T]	1.74		
Integrated field [Tm]	4.44		

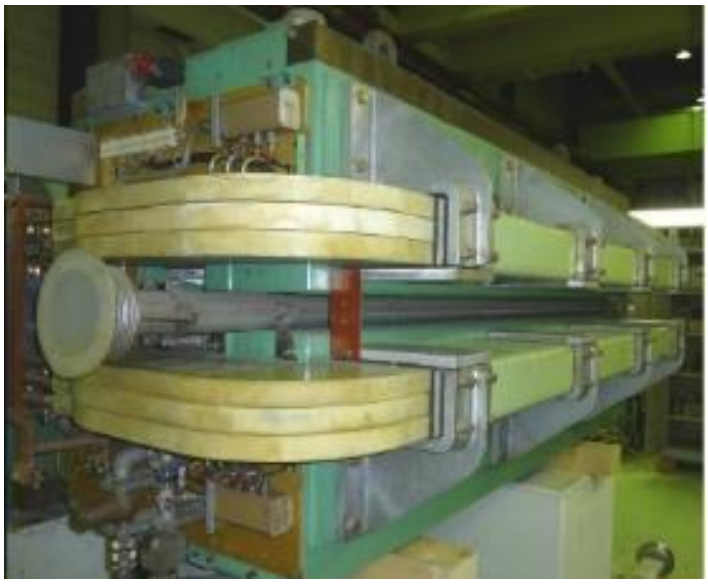

Fig. 4-2: MCB magnet.

4.1.2.1 New M100 L and M200 L bending magnets

These two new families are laminated versions of the present M100 [5] and M200 [6] built in the 1960s, and are mainly used in the experimental areas and where large apertures are needed. The present massive yoke design can vary its aperture gap between 110 and 200 mm by adding steel plates between the two half-yokes. This option of gap modification cannot be applied easily to laminated yokes. A schematic representation of these magnets can be found in Fig. 4-3. The most important constraints for these two designs were the overall sizes to fit in the layout, and the number of turns to match the characteristics of the power supplies. In the first stage of the project, it was foreseen that the existing coils could be kept but, due to their too high inductance, the number of turns had been reduced. The range of integrated fields required for the M100 L is 1.5 Tm and from 2.5 to 3 Tm for the M200 L (see Table 4-2).

Table 4-2: M100 L – M200 L bending magnet characteristics.

CERN code	**PXMBXHFHWP**	**PXMBXGFHWP**
Short name	M100 L	M200 L
Number of magnets	2 + a set of coils	6 + a set of coils
Aperture [mm]	110	140
Iron length [mm]	1 000	2 000
Total length [mm]	1 730	2 730
Total width [mm]	1 820	1 820
Total height [mm]	1 300	1 300
Weight [kg]	17 100	33 000
Nominal current [A]	985	1 300
Resistance [mΩ]	58.1	83
Inductance [mH]	280	428
Power at nominal current [kW]	56.4	139
Delta P nominal [bar]	3	7.1
Nominal cooling flow [l/min]	50.4	67.2
Number of turns per pole	96	96
Nominal field [T]	1.646	1.716
Integrated field [Tm]	1.821	3.585

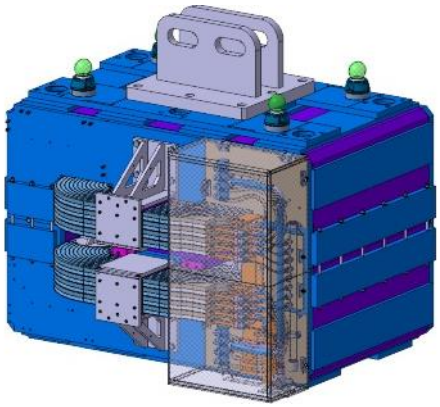

Fig. 4-3: New M100 L 3D CAD view.

4.1.3 Quadrupole magnets

Seven types of quadrupoles are needed for the EA renovation, as illustrated in Fig. 4-4. Available laminated designs, the QDS [7], QFS [8], and QFL [9], are families built in the 1970s for the ISR beam transfer lines, as with the MCB. Like the M100 and M200, the present Q100 [10] and Q200 [11] will be replaced by laminated versions: Q100 L [12] and Q200 L [13]. New Q74 L [14] and Q120 C [15] will substitute the actual magnets, only used in the EA, due to their poor state and high radiation activation.

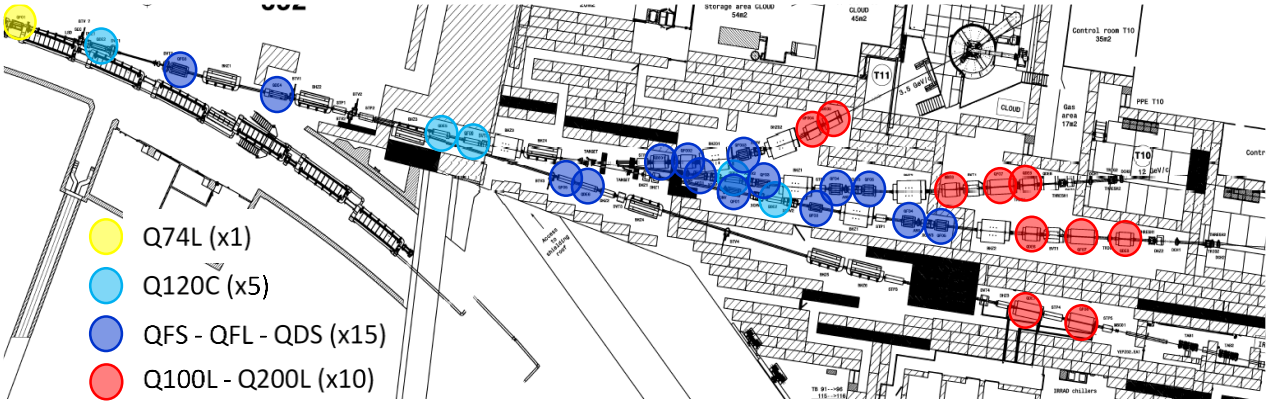

Fig. 4-4: Quadrupole magnet EA layout.

4.1.3.1 QDS – QFS – QFL quadrupole magnets

The required quantity of magnets is covered by the spare ones stored. They will be tested, disassembled, cleaned, improved, reassembled, certified, and magnetically measured. They are also commonly used at CERN; 57 units are currently in operation mainly in the transfer lines and experiment areas. The maximum required integrated gradients are 10.7, 12.2, and 19.5 T for the QDS, QFS, and QFL, respectively (see Table 4-3). In Fig. 4-5 there are photos of these magnets assembled.

Table 4-3: QDS – QFS – QFL quadrupole magnet characteristics.

CERN code	**PXMQNDCTWP**	**PXMQNEGTWP**	**PXMQNEFTWP**
Short name	QDS	QFS	QFL
Number of magnets	4 + 1	8 + 1	3 + 1
Aperture [mm]	91	100	
Iron length [mm]	820	800	1 200
Total length [mm]	1 080	1 080	1 481
Total width [mm]	600	844	
Total height [mm]	900	1 000	
Weight [kg]	1 600	2 900	4 200
Nominal current [A]	500		
Resistance [mΩ]	59	62	96
Inductance [mH]	45	80	120
Power at nominal current [kW]	15	16	24
Delta P nominal [bar]	5		
Nominal cooling flow [l/min]	8	8	12
Number of turns per pole	34	41	
Nominal gradient [T/m]	19.2	18.9	
Integrated gradient [T]	16.3	15.7	23.2

Fig. 4-5: QDS – QFS – QFL magnets.

4.1.3.2 New Q100 L – Q200 L quadrupole magnets

These two new families are laminated versions of the Q100 and Q200 built in the 1960s and mainly used in the experimental areas and where large apertures are needed. The current designs have massive yokes and coils that are in poor shape. The reuse of the current coils is not foreseen for reasons of reliability. Both families have the same cross-section and only the iron length differs: at one (Q100 L) and two metres (Q200 L). The maximum required integrated gradients are 11.8 and 20 T for the Q100 L and Q200 L, respectively (see Table 4-4).

As with the Q100 L and Q200 L designs (Fig. 4-6), the more important constraint for the design was the overall length to fit in the layout. The width can be increased, as long as the actual supports can be used, but not the length. The iron lengths will be identical as in the present designs, consequently the coil and mechanical designs have to be adapted.

Table 4-4: Q100 L – Q200 L quadrupole magnet characteristics.

CERN code	**PXMQNEVTWP**	**PXMQNFKTWP**
Short name	Q100 L	Q200 L
Number of magnets	5 + a set of coils	
Aperture [mm]	200	
Iron length [mm]	1 000	2 000
Total length [mm]	1 460	2 480
Total width [mm]	1 200	
Total height [mm]	1 200	
Weight [kg]	7 000	11 500
Nominal current [A]	800	
Resistance [mΩ]	158	249
Inductance [mH]	166	320
Power at nominal current [kW]	101	159
Delta P nominal [bar]	4	7
Nominal cooling flow [l/min]	86	91
Number of turns per pole	70	70
Nominal gradient [T/m]	11.5	
Integrated gradient [T]	12	24

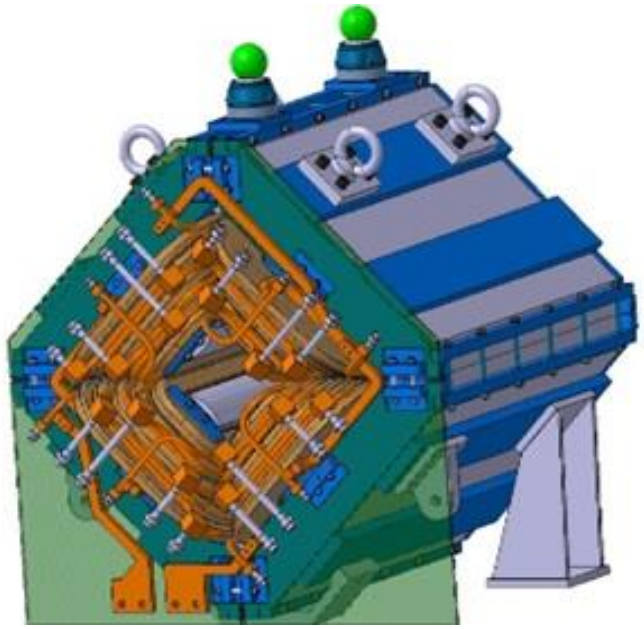

Fig. 4-6: New Q100 L 3D CAD view.

4.1.3.3 New Q74 L and Q120 C quadrupole magnets

The Q74 [16] is the first magnet of the F61 extraction line and the place available is limited by the space between the magnet vacuum chamber and the PS ring vacuum chamber, see Fig. 4-7. Only a Collins quadrupole shape can be designed to avoid using space intended for the magnetic return yokes. The required integrated gradient is 31 T (see Table 4-5).

The present Q120 [17] magnets, although laminated, have to be substituted by new magnets due to the high level of radiation accumulated over a 12-year period in the primary area. As for the Q74, these magnets are placed close to the line separations, between F62 and T08, and therefore will be Collins shaped. The required integrated gradient is 19 T (see Table 4-5). For these two designs, we take advantage of the need for replacement to improve the pole shapes, coil configurations, and cooling system to have a higher reliability.

Table 4-5: Q74 L and Q120 C quadrupole magnet characteristics

CERN code	**PXMQNCL8WP**	**PXMQNEL8WP**
Short name	Q74 L	Q120 C
Number of magnets	1 + 1	5 + 1
Aperture [mm]	50	100
Iron length [mm]	700	1 200
Total length [mm]	1 000	1 360
Total width [mm]	225	415
Total height [mm]	420	600
Weight [kg]	600	1 939
Nominal current [A]	800	600
Resistance [mΩ]	75	600
Inductance [mH]	1.7	48
Power at nominal current [kW]	821	48.2
Delta P nominal [bar]	6	6.4
Nominal cooling flow [l/min]	26	31
Number of turns per pole	16	33
Nominal gradient [T/m]	47	18.4
Integrated gradient [T]	33	22.9

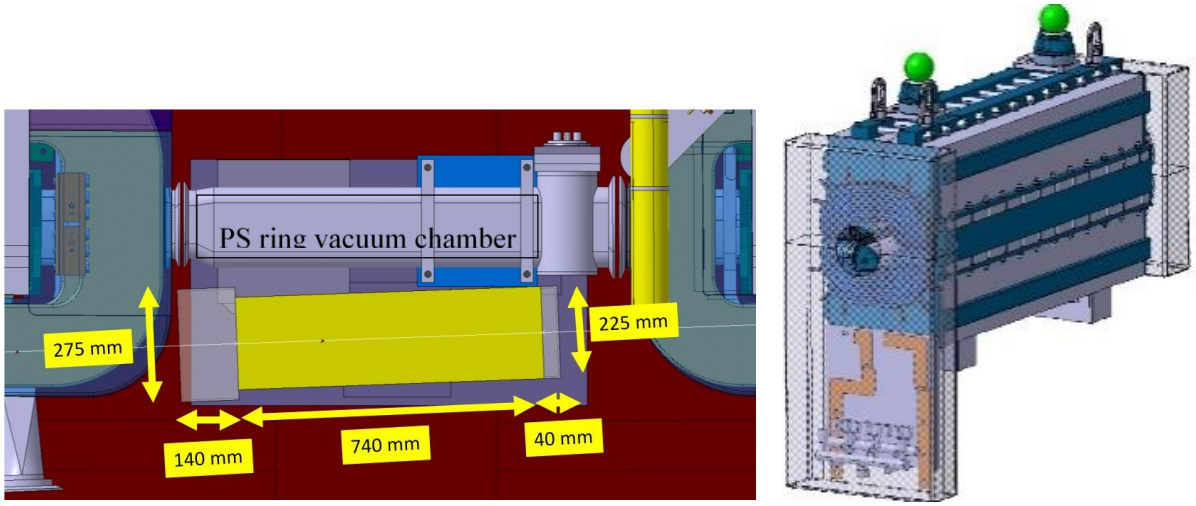

Fig. 4-7: Left: top view of Q74 maximum overall dimensions; right: new Q120 C 3D CAD view.

4.1.4 Corrector magnets

Two types of correctors are needed for the EA renovation (see Fig. 4-8). Some requirements could have been fulfilled with the existing massive magnets such as the MEA19 [18] or MDX [19] but, due to the eddy currents, the delay between field and current is at the limit of the cycle time required. The lengths available for these two designs are limited by the new layout of the beamlines and challenging compromises have been made between the magnet design and beam optic.

Fig. 4-8: Corrector magnets EA layout.

4.1.4.1 New CR200 and MDX L corrector magnets

The CR200 [20] corrector (Fig. 4-9) is a large aperture magnet tightly fitted between two quadrupoles. Its design has been optimized to minimize the magnetic coupling between these magnets with a three-dimensional study [21]. With the first requirement of a large aperture, at 150 mm, the CR200 corrector was not feasible. Therefore, the aperture was reduced from 150 to 100 mm. Even with this aperture reduction, the distance available between the adjacent magnets is at the limit of a realistic magnet's overall length. The magnetic coupling between these magnets has been studied, and proven to be negligible in terms of integrated magnetic homogeneity (see Table 4-6).

The new MDX L 150 [22] is a laminated version of the actual MDX. As the M100 and M200 are massive, the aperture of the actual MDX can vary its gap between 52 and 120 mm by adding steel plates between the two half-yokes. This option of gap modification cannot be applied easily to laminated yokes. A few different gaps were foreseen but, in order to have as few as possible different designs, it was decided to do only one type with an aperture of 150 mm (see Table 4-6).

Table 4-6: CR200 and MDX L corrector magnet characteristics.

CERN code	PXMCXCEHWP	PXMCXCFHWP
Short name	CR200	MDX L 150
Number of magnets	4 + 1	8 + 1
Aperture [mm]	100	150
Iron length [mm]	200	400
Total length [mm]	500	655
Total width [mm]	830	730
Total height [mm]	700	680
Weight [kg]	910	1 100
Nominal current [A]	600	240
Resistance [mΩ]	40.8	240
Inductance [mH]	22	300
Power at nominal current [kW]	14.7	221
Delta P nominal [bar]	10	10
Nominal cooling flow [l/min]	7.1	9
Number of turns per pole	64	180
Nominal field [T]	0.9	0.7
Integrated field [Tm]	0.28	0.36

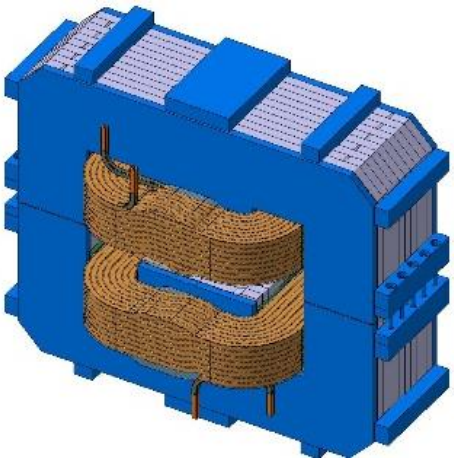

Fig. 4-9: New CR200 3D CAD view.

4.2 Power converters

4.2.1 East Area present situation

The EA powering is presently supplied by 65 power converters that are located in Buildings 251 and 263. There are 47 power converters in Building 251 and 18 power converters in Building 263.

A study has been performed in 2012 [22][23][24] by the electrical power converters group showing that the energy consumption of East Area could be reduced from 11 GWh to 0.6 GWh per year after Long Shutdown 2 (LS2). A significant part of this saving could be obtained by using a cycling magnet current, hence recovering and storing the magnet energy after each physics operation. The study also highlighted the possibility of self-funding part of the upgrade program, notably the power electronic converters, with a depreciation period of five years for this investment.

4.2.2 East Area future layout and operation

The future beamlines (as defined in Section 2.1) of EA consist of 58 magnets of 12 different types (see Fig. 4-10) to be powered by 61 power converters.

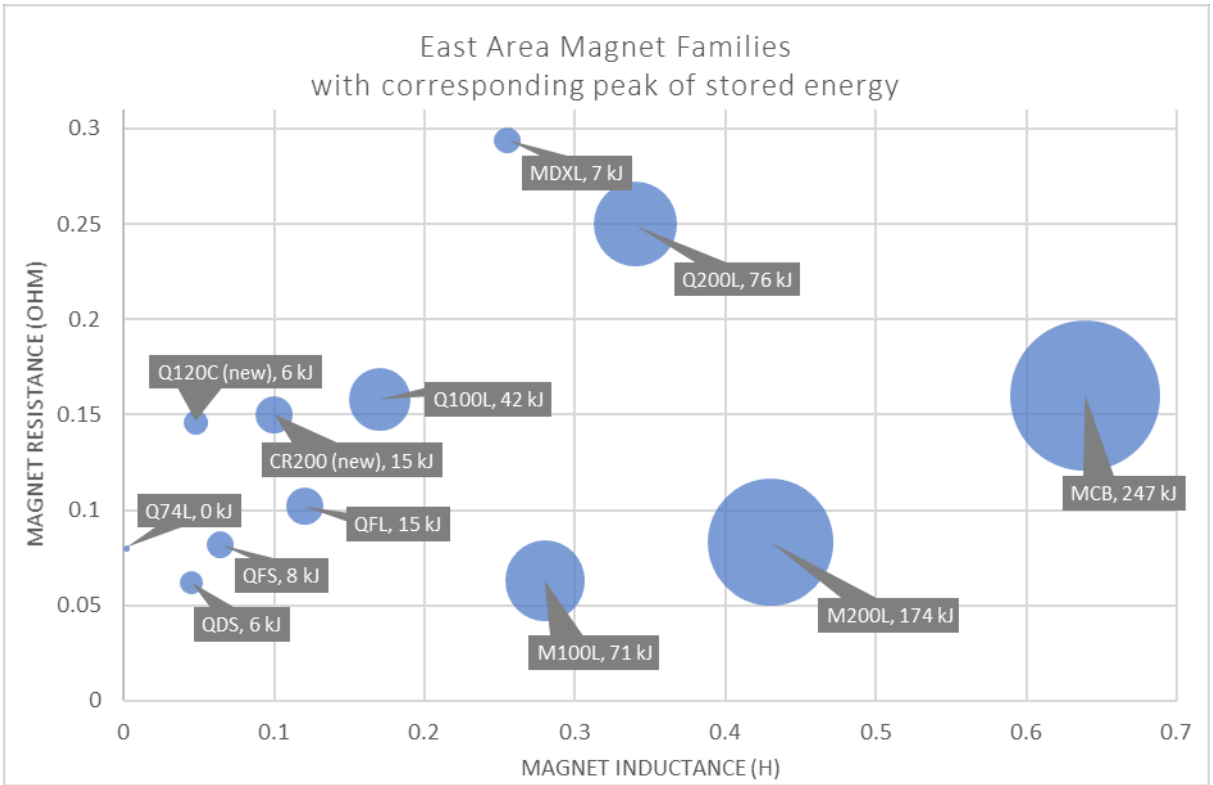

Fig. 4-10: The magnet map of East area. The axes correspond to the inductance and resistance of each magnet while the bubble size represents the peak stored energy (and hence the size of the magnet).

The beamlines and key bending elements are depicted in Fig. 4-11.

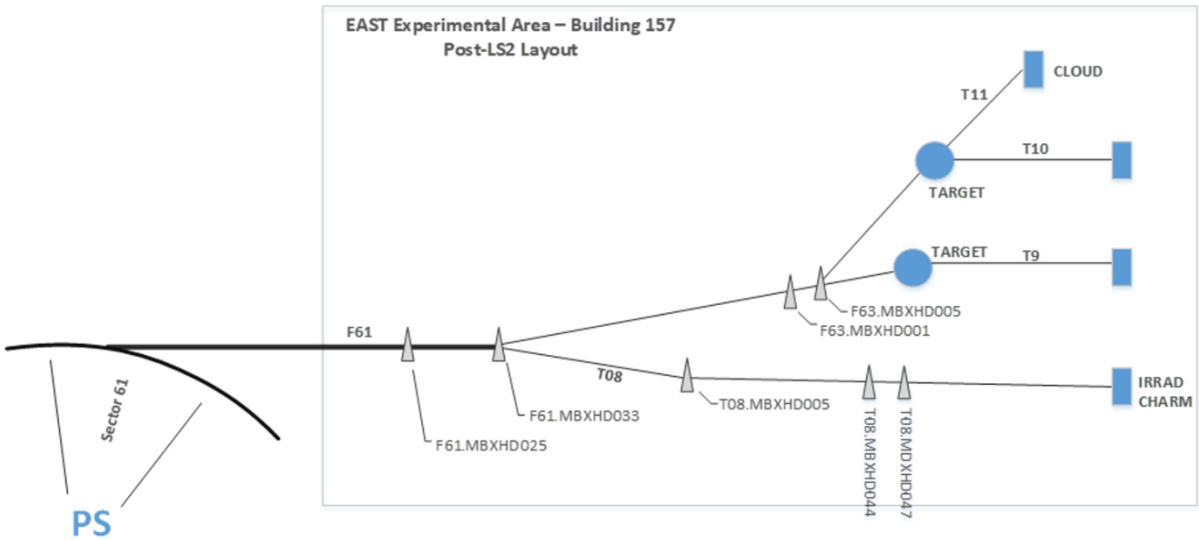

Fig. 4-11: The proposed East Area layout after LS2.

The new layout will operate with a cycling current in all magnets in order to save energy. The form of the cycle will be as illustrated in Fig. 4-12.

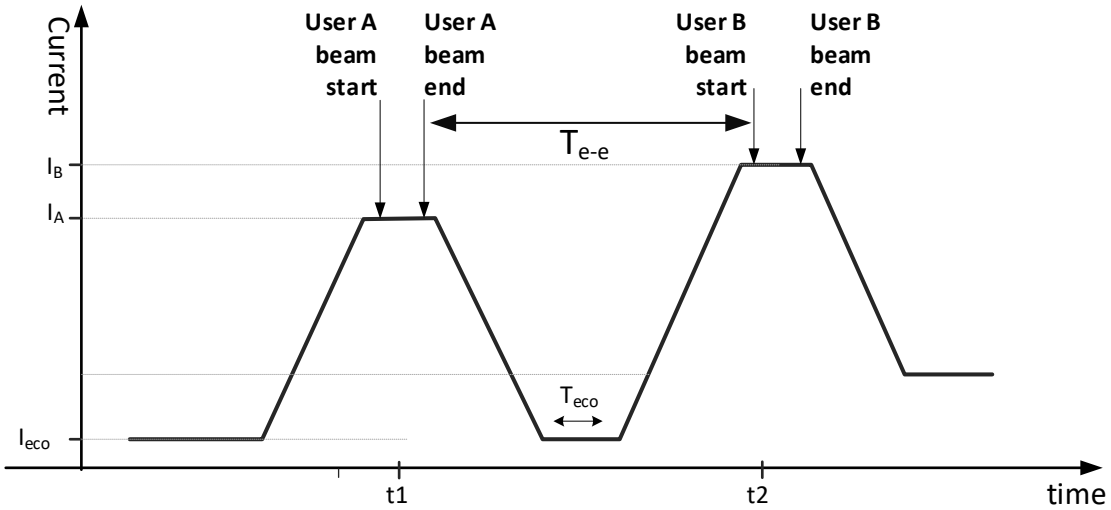

Fig. 4-12: Magnet current cycle in the new EA beamlines. The figure illustrates two successive beam extractions; one for user A and a second for user B. The typical duration of each beam extraction is up to 400 ms and the time between two successive extractions (Te-e) is 1.93 seconds minimum. Certain lines will cycle with a 2.4 s period whereas others will have a 4.8 s period.

The duty cycle of the EA transfer lines will remain as it currently is at approximately 3.15 seconds (7 extractions of an approximate extraction duration of 470 ms each) in a typical super-cycle of 46.8 seconds. This implies a maximum duty cycle of 7% for the power converters (the time duration in a supercycle while extraction to the East Area takes place).

The cycle characteristics appear in Fig. 4-13. The extraction time lasts 400 ms with a spill start and end time tolerance of 10 ms on either side. Prior to the beam extraction, there is a maximum of 50 ms of current settling into the magnet. The precise requirements are discussed in Refs. [25][26].

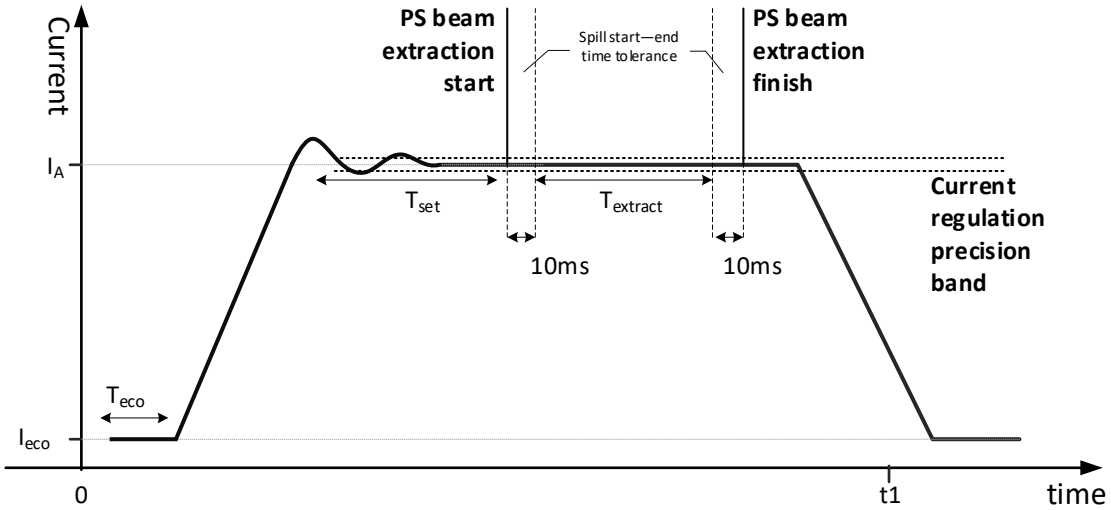

Fig. 4-13: Magnetic cycle characteristics. The settling time (Tset) allows for the current (and corresponding magnetic field) to settle to a value within the required precision. A tolerance of 10 ms is defined for the start and stop of the beam spill and hence for the beam extraction interval.

The root mean square (RMS) ratings of each circuit and losses in each circuit are listed in the following tables.

4.2.3 Powering solution

The present EA powering employs technology from the 1950s. Self-commutated thyristor converters were the state of the art at the time of construction and have been reliably supplying the East Area magnets for a very long time.

The proposed powering solution is based on the SIRIUS power converter family. The SIRIUS family (refer to Table 4-7) has been developed especially for Accelerator Transfer Line applications and performs magnet energy recovery after each magnetic cycle.

Table 4-7: Variants of the SIRIUS converter family.

Family	Type	Configuration	Grid supply (RMS values)	Output continuous	Output cycling peak
SIRIUS	**S**	Single module	400V/32A	200A/15kW	±450V/±450A
SIRIUS	**2P**	2 modules in parallel	400V/63A	400A/30kW	±450V/±900A
SIRIUS	**4P**	4 modules in parallel	400V/125A	800A/60kW	±450V/±1 800A
SIRIUS	**4P+**	4 modules in parallel with additional energy storing capacitors	400V/125A	800A/60kW	±450V/±1 800A

The power converter employs a diode rectifier (see grid supply in Fig. 4-14) followed by a boost switching regulator acting as a power network current flow controller. An intermediate energy storage stage supplies or absorbs the instantaneous peak power from the power converter load. Finally, the DC/DC magnet supply unit performs the high-precision current regulation in the electro-magnet load.

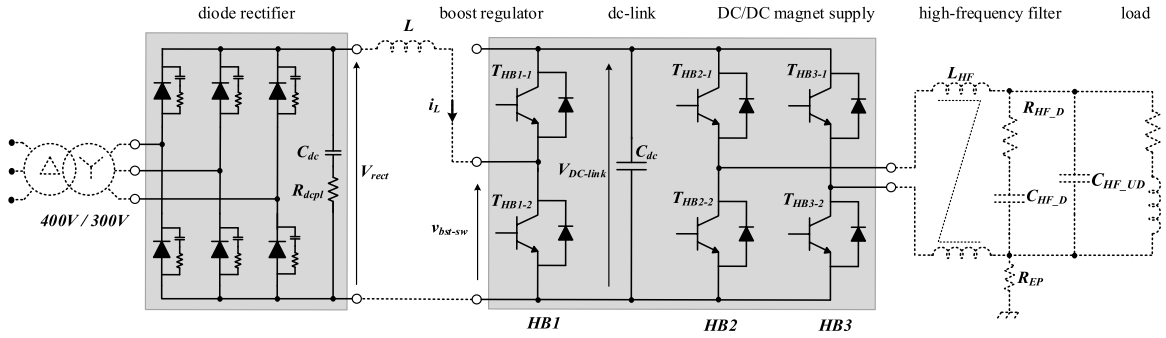

Fig. 4-14: Schematic of a SIRIUS S power converter module connected to a magnet.

SIRIUS 2P has been designed with fast cycling loads in mind and is able to recover magnet energy of up approximately 65 kJ. The power converter has been designed for a cycling rated voltage and current of 450 V and 900 A (with an RMS current of 400 A). However, it can supply a magnet with continuous (DC) output current with a current of up to 400 A, provided that the resistive magnet losses do not exceed the 30 kW input RMS power rating of the power converter. The unit can therefore provide a constant RMS power of 30 kW to the load whereas the peak cycling power deliverable to the magnet is 405 kW. The grid supply unit limits the power taken from the power network to 20 kVA with a 63 A/400 V three-phase line voltage. This unit serves to improve power quality towards the power network by limiting the input power fluctuation.

The SIRIUS power converter family (Fig. 4-15) has been designed mainly for cycling applications in transfer lines. Cycling applications tend to be more demanding on power electronic components as they trigger a number of effects, such as electromechanical stressing and thermal stressing (in particular in semiconductors and capacitors). A number of studies have been completed to that end to validate the design in terms or lifetime and safety, as listed in Table 4-8.

Table 4-8: References to studies performed during the development of SIRIUS.

Study	Relevant components	References
Accelerated aging testing	Electrolytic capacitors	[27][28]
Thermal cycling	Semiconductor switches (IGBTs)	[29]
Energy recovery	Control loops	[30][31][32]
Electrical Safety	Electrolytic capacitors, semiconductor power stack	[33]

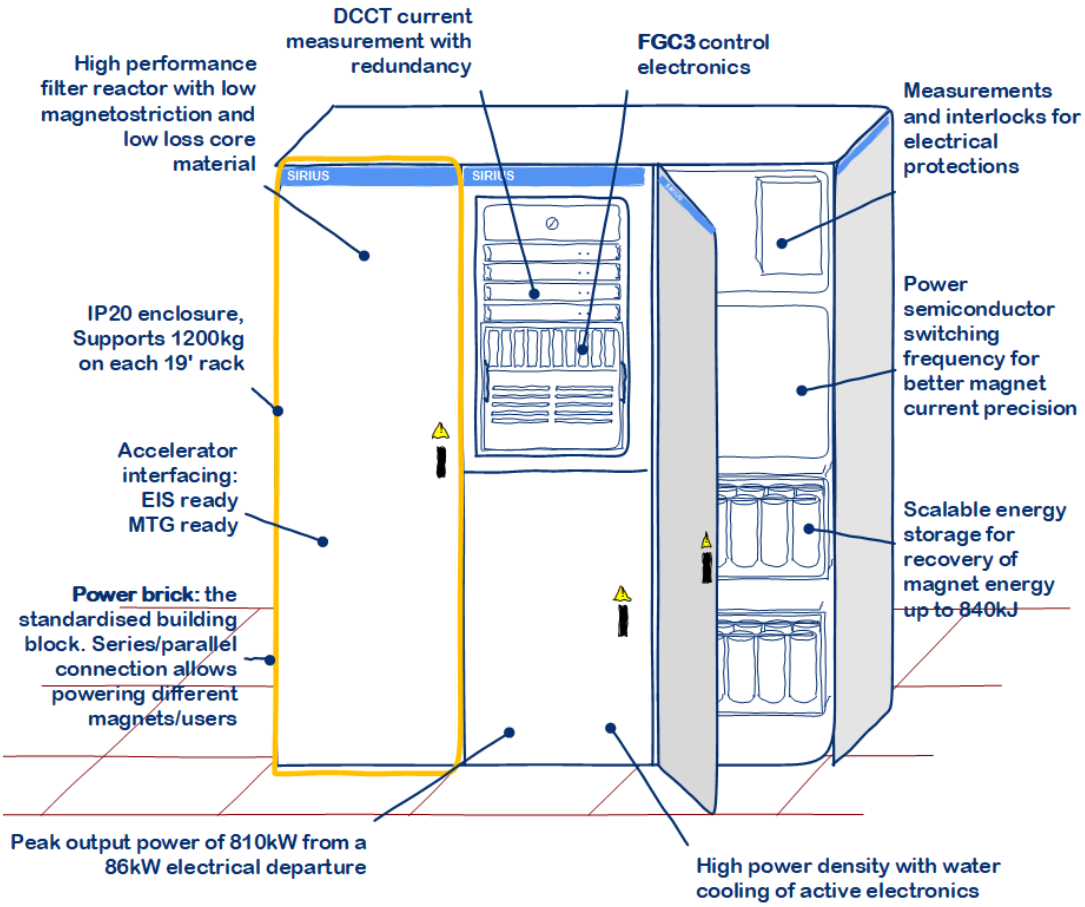

Fig. 4-15: Features of SIRIUS power converters family.

4.2.3.1 Spare converters and spare parts

Three power converters, one 2P and two 4P+, will be available in the East Area in case of malfunction of any of the operating power converters. All three can operate for a SIRIUS S in case of need. Interconnection of spare converters with the magnet load will be made by means of power cables that will be temporarily laid on the floor for the duration of spare converter operation.

4.2.3.2 MTG requirements

The machine timing generation (MTG) system is a programmable logic controller (PLC) based system that monitors the status of different components of the accelerators and reconfigures the supercycle of the machine accordingly. In the East Area, two power converters that direct the beam to the beam dump will be interfaced with the MTG system (see Table 4-9). Following a change of strategy of the Power Converters Group post-LS2, the EA power converters will not be interfaced to the MTG through a direct cable connection to the power converter. Instead, the MTG subscribes to a converter property that notifies the converter state.

Table 4-9: Power converters connected to the MTG system.

Power converter name	MTG interface
RPAEK.251.F61.RBXHD025A	Software (by subscription to FGC property)
RPAEK.251.F61.RBXHD025B	Software (by subscription to FGC property)

4.2.3.3 Elements important for safety (EIS) requirements

Two circuits will be part of an EIS-beam chain. In the case of a fault in one of the EIS power converters (see Table 4-10), a spare scheme has been proposed with a safe to operate switch-over system that obliges the operator to enable the EIS chain on the spare converter prior to connecting it to the EIS magnet [34].

Table 4-10: Power converters connected to the EIS system.

Power converter name	Type of EIS
RPAEK.251.T8.MBXHD044	Beam
RPAEK.251.T8.MBXHD047	Beam

4.2.3.4 Energy saving

A new energy saving mode has been conceived for the SIRIUS converters installed for the transfer lines. The algorithm runs in the FGC controller of the power converter. The operation requirements, such as the current value and extraction, of each physics user are processed together with the circuit parameters and a current waveform with the minimum possible RMS value is calculated prior to each magnetic cycle [35]. This process is transparent for the operation and relies on a timing event received from the gateway by the FGC controller over the FGCEther network. The timing will arrive 1.2 second prior to the extraction start instance so that enough time is available for reaching the user current, even for magnets with a large time constant.

4.2.3.5 Control facility

A control room will be constructed that will allow technical personnel to operate in a quiet environment for remote control and maintenance checks of the power converters.

4.3 Vacuum system description

The vacuum system of the EA will be renovated in the frame of the EA Renovation project: it includes the hardware (vacuum chambers, pumps, gauges, etc.) and the remote control system.

The current vacuum system installed in the East Area is a very old and unreliable system. The pumps are old, with a volume flow rate of 16 m^3/h and with a very complex maintenance frequently required. Furthermore, the control system only shows the vacuum level (which is not available remotely) but is does not show the pumps' status.

For these reasons, it has been decided to change and to upgrade the entire vacuum system of the East Area, taking as a reference model the system installed in the North Area. The proposed vacuum system is in line with other vacuum systems at CERN, and has been optimized to minimize intervention time and exposure to radiation.

The system is equipped with on-line supervision to be monitored and controlled from the CERN Central Control room (CCC) and remotely from a PLC platform. With the new chosen components, it is possible to produce a 5×10^{-3} mbar vacuum.

The new vacuum system is divided into 5 sectors:

i) Sector 1: from the BTV in F61 line until the 1st bending, in green in Fig. 4-16.

ii) Sector 2: from the 1st bending to the 3rd bending in F62 and to the proton IRRADiation facility (IRRAD) in T08, in yellow in Fig. 4-16.

iii) Sector 3: T09 line, in red in Fig. 4-16 .

iv) Sector 4: T10 line, in pink in Fig. 4-16.

v) Sector 5: T11 line, in grey in Fig. 4-16.

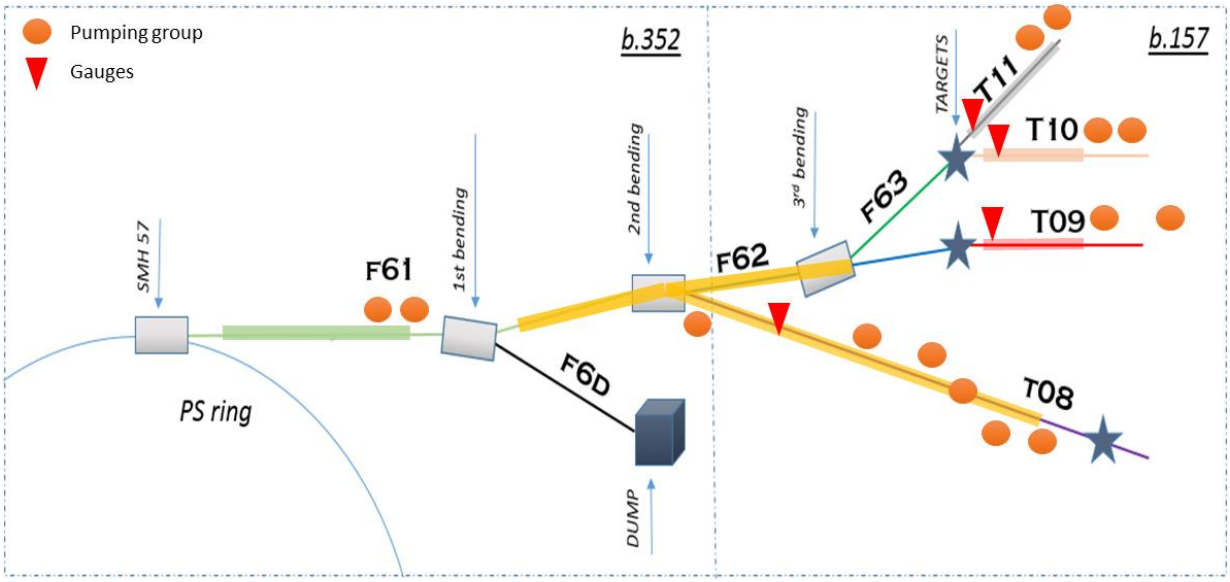

Fig. 4-16: Vacuum sectors of the East Area.

The new vacuum chambers are all in non-magnetic stainless steel (304L or 316L). Their standard size is DN219, but at some points, they have different dimensions to adjust to the beam's radius and they depend on the outer equipment available space (magnets, collimators, etc.). The flanges used are conflate with metallic seals. The windows for each sector are made of mylar or aluminium and their thickness depends on the beam's intensity and particle type.

Some cut-off manual section valves will be installed on the vacuum lines in order to isolate a part of the vacuum sector in case maintenance is needed on a piece of equipment.

4.3.1 Pumping groups

The new EA vacuum system has 14 pumping groups and four gauges located at different positions in the beamline. Each pumping group is made of valves, a gauge, a monitor, and a pump. The singular gauges are just to control the vacuum level in the system. The general layout and structure can be seen in Fig. 4-17 and more information is available in Ref. [36].

Inside the primary and mixed areas, no vacuum groups are installed because these areas are the most radioactive ones. In this way, it is possible to reduce the radiation damage to the pumps and the electrical systems, but also the exposure of the workers during maintenance. Inside the primary and mixed areas only four gauges are installed to monitor the vacuum level.

In some cases, the most critical vacuum groups (of more difficult access) will have two pumps mounted in parallel in order to have a redundant backup solution in case a fault occurs.

Fig. 4-17: Layout of the new vacuum system

4.3.2 Vacuum controls

The vacuum control system consists of a Siemens 1500 PLC, three sets of input/output (I/O) stations with a Profinet communication protocol and five total pressure gauge controller (TPG300), each with a set of Profibus, Pirani cards to receive the signal from the groups pumping. A supervisory control and data acquisition (SCADA) system based on the WinCC Open Architecture (OA) forms the remote interface with the users. The objective is to avoid radiation in the interventions on the pumping groups and on the Pirani gauges when the East Area receives the PS beam. The SCADA application will be implemented in the complex PS framework to include the East Area synoptic.

4.4 Beam intercepting devices

4.4.1 Introduction

The EA Beam Stopper Consolidation started before the Long Shutdown 1 (LS1). During LS1, a general maintenance was performed, including urgent interventions on the beam stoppers, such as the replacement of the compressed air distribution and the switches. During LS2, the layout of the beamlines will be modified. This will affect the layout and functionality of the beam stoppers, stopper dumps, and multitargets.

– Beam stoppers, stopper dump:

in particular the basic layout of the North branch will be revised completely. In the present beam layout, the primary protons that did not interact in the North multi-target are stopped in the T09 beam stoppers in case of access to T09. In the new layout those protons will be stopped in a fixed dump and the T09 stopper dumps will only see low-intensity secondary beams.

– Targets:

the new layout requires the installation of two multi-targets, one to produce the T09 beam and the second to produce T10 and T11 beam. The special target used in CERN High energy AcceleRator Mixed field facility (CHARM) is not affected by the renovation.

4.4.2 Situation post LS2

4.4.2.1 Introduction

The validation work of the current beam stoppers [37] showed that their absorbing blocks are not suitable for present and future beam scenarios. Based on the experience gained over past years, a functional specification was drafted in order to set the requirements (see Table 4-11) for the design and operation of the new PS complex beam stoppers, including the East Area [41]. This stopper design will be used throughout the PS complex.

Table 4-11: Summary of requirement for new PS beam stoppers.

Life-time	Until 2048
Thermo-mechanical	< 15 repeated pulses
Material limit	$\sigma_e < \sigma_y(T)$ – von-Mises criterion (ductile materials)
Beam attenuation	Multiples of λ dependent on each PS line
Beam parameters	26 GeV/c, 2.3×10^{13} ppp (critical)
Beam passage	Ø 156 mm
Vacuum	5×10^{-3} mbar (EA) – 5×10^{-8} mbar (PS)
Integration	Flange-to-flange (< 884 mm)
Alignment	±2 mm (core-beam centre), ±0.5 mm flange centres (two chambers)
	Plug-in system, manual service connectors
Maintainability	Fully modularized
	Lock for OUT-BEAM core
Manufacturing	Rough core surface (passive cooling)
Fail-safe	Yes
Safety	at least two beam stoppers at each line (except secondary lines)

4.4.2.2 Stopper core design

The description, calculations, and design of the core are detailed in Ref. [42]. It has a diameter of 200 mm divided into four Inconel718 slices and one CuCr1Zr 400 mm thick slice. Figure 4-18 presents the different materials of the core design.

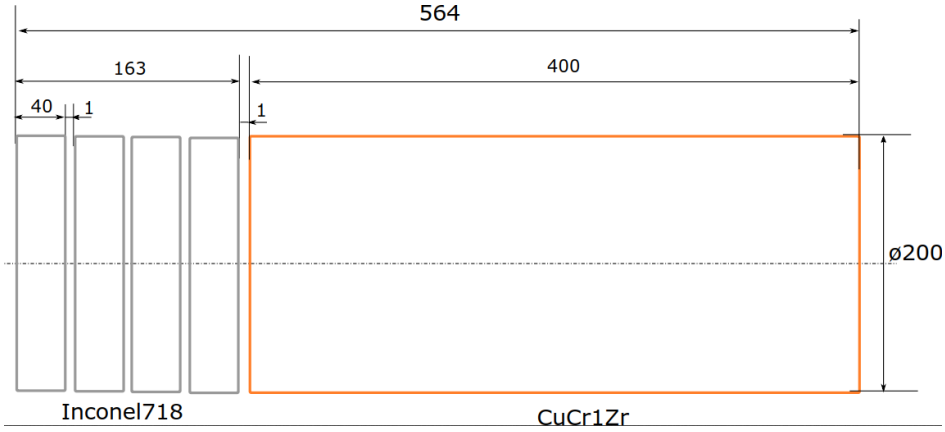

Fig. 4-18: Schematic representation of the core of the new PS beam stopper.

The core was designed to withstand 15 repeated pulses of the most critical beam in the PS complex (High Luminosity Large Hadron Collider (HL-LHC) beam, 26 GeV/c, 2.3×10^{13} protons per pulse). It is passively cooled through radiation to the vacuum chambers and heat conduction through supports.

The primary beam attenuation of the core is 3.8 λ at 26 GeV/c, which corresponds to 97.8% of the incoming protons.

4.4.2.3 General description of the new beam stopper and stopper dump

Figure 4-19 shows the 3D model of the new beam stopper. This equipment is totally independent of neighbouring mechanical equipment, with its own vacuum chamber, mechanism, plug-in, and support systems. The new beam stopper has a weight of 550 kg and a height of 1 600 mm.

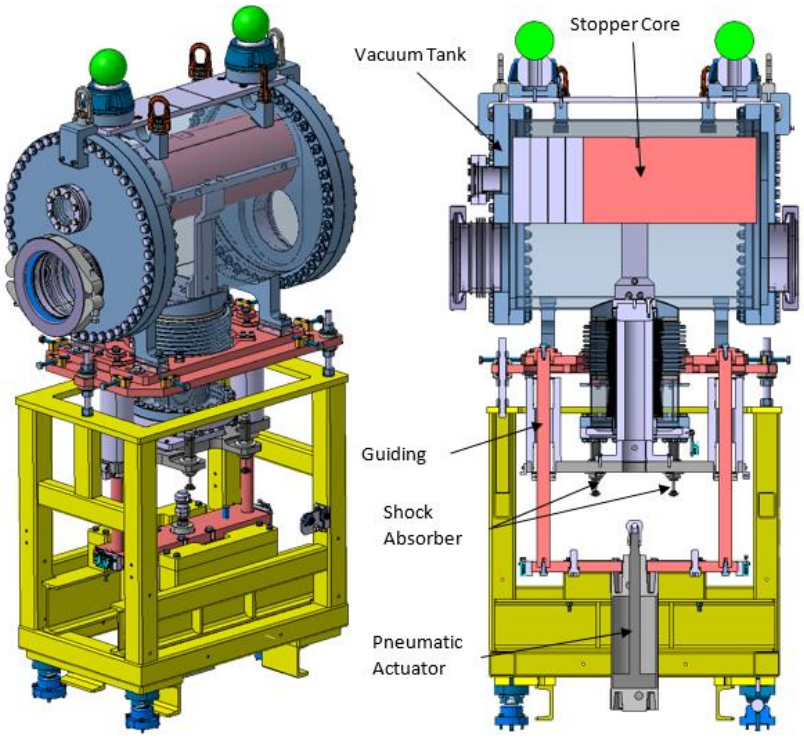

Fig. 4-19: Three-dimensional view and cut view of the new beam stopper.

The final design is composed of the following sub-systems, as shown in Fig. 4-20: the stopper core, which is held by a fork. The fork is welded to the bellows, which are themselves connected to the base plate. The shock absorbers and ball bearings are fixed onto this plate as well. The pneumatic actuator is also fixed below this plate.

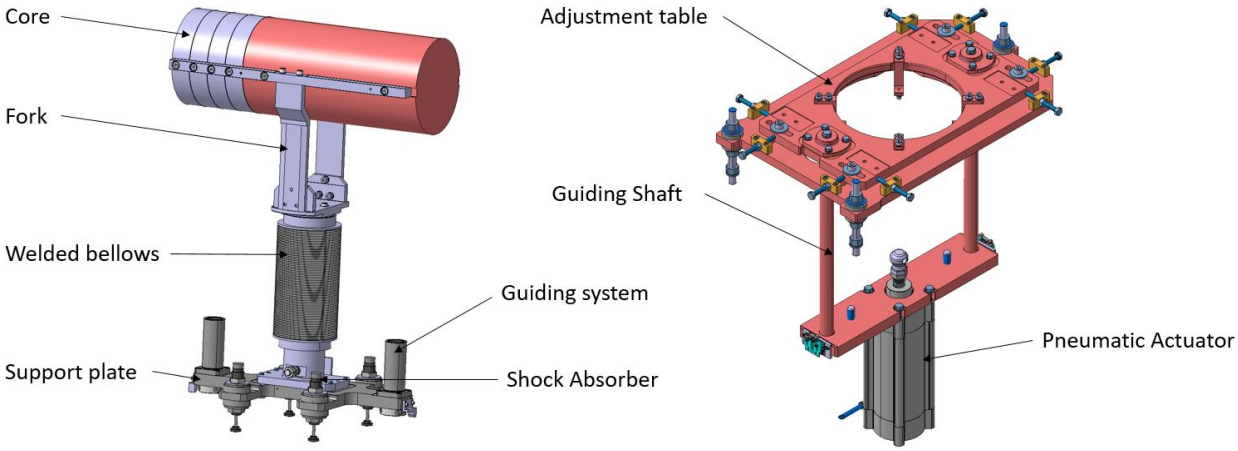

Fig. 4-20: Details of the stopper moving mechanism.

The pressurized pneumatic cylinder keeps the core in the OUT-BEAM position. The design has been calculated to work with a pressure of 4 bars. This margin allows for an increase of the pressure in case of

friction. When it is de-pressurized, the core falls in the IN-BEAM position. The support plate is damped through shock absorbers on the frame (see Fig. 4-19).

Whenever members of personnel want or are forced to access a downstream area or in fail-safe situations [43], the core needs to move to the IN-BEAM position. The assembly slides in the guiding system vertically.

On the top of the guiding shaft there is an adjustment table for surveying, which supports the tank, as shown in Fig. 4-21.

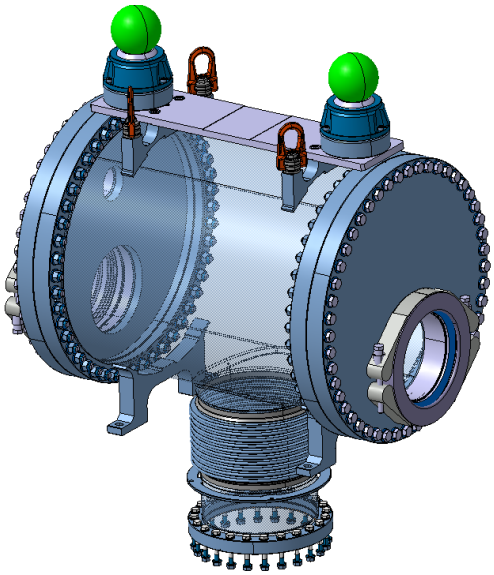

Fig. 4-21: Dedicated vacuum chamber for the beam stoppers.

4.4.2.4 Multitarget

The new multitarget design can be found in Fig. 4-22 and is composed of five different sub-systems:

i) Aluminium profile chassis.

ii) X–Y motorization.

iii) Target arm with a beam screen.

iv) Camera.

v) First Plug-in support.

The major change from the first multitarget is the modification of the adjustment system on the target arm. It allows surveys to be more precise and it is faster to align the target. Furthermore, a lower plugin position of the chassis was added in case the entire multitarget has to be removed. The motorization has also changed to better manage the spare pool.

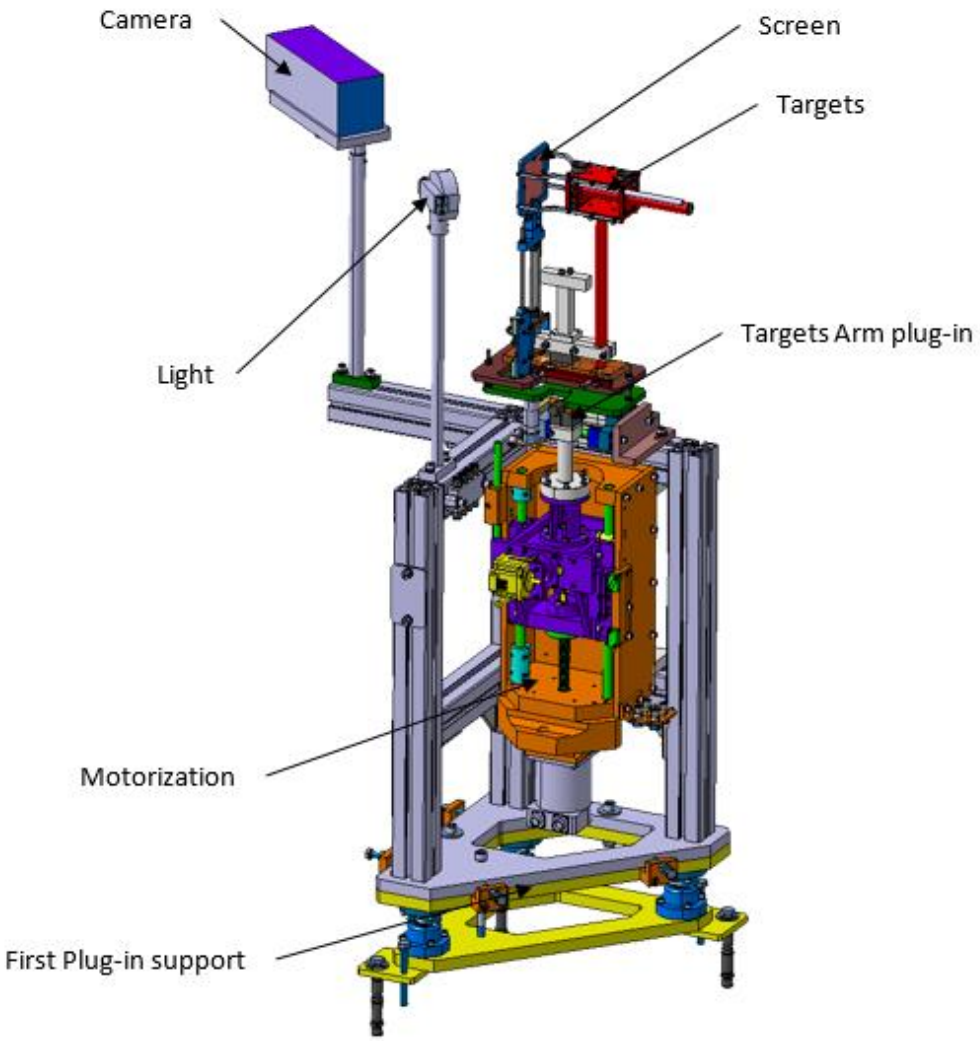

Fig. 4-22: Multitarget new design.

4.4.2.5 East Area integration

In this new configuration (Fig. 4-23), five beam stoppers will be installed on the F61 and another five on the T8 line. This number of stoppers on this line is due to the radiation protection requirements for the beam attenuation and the facility of access to the downstream experimental area. Each secondary beamline is protected by one stopper dump each (T09, T10, T11).

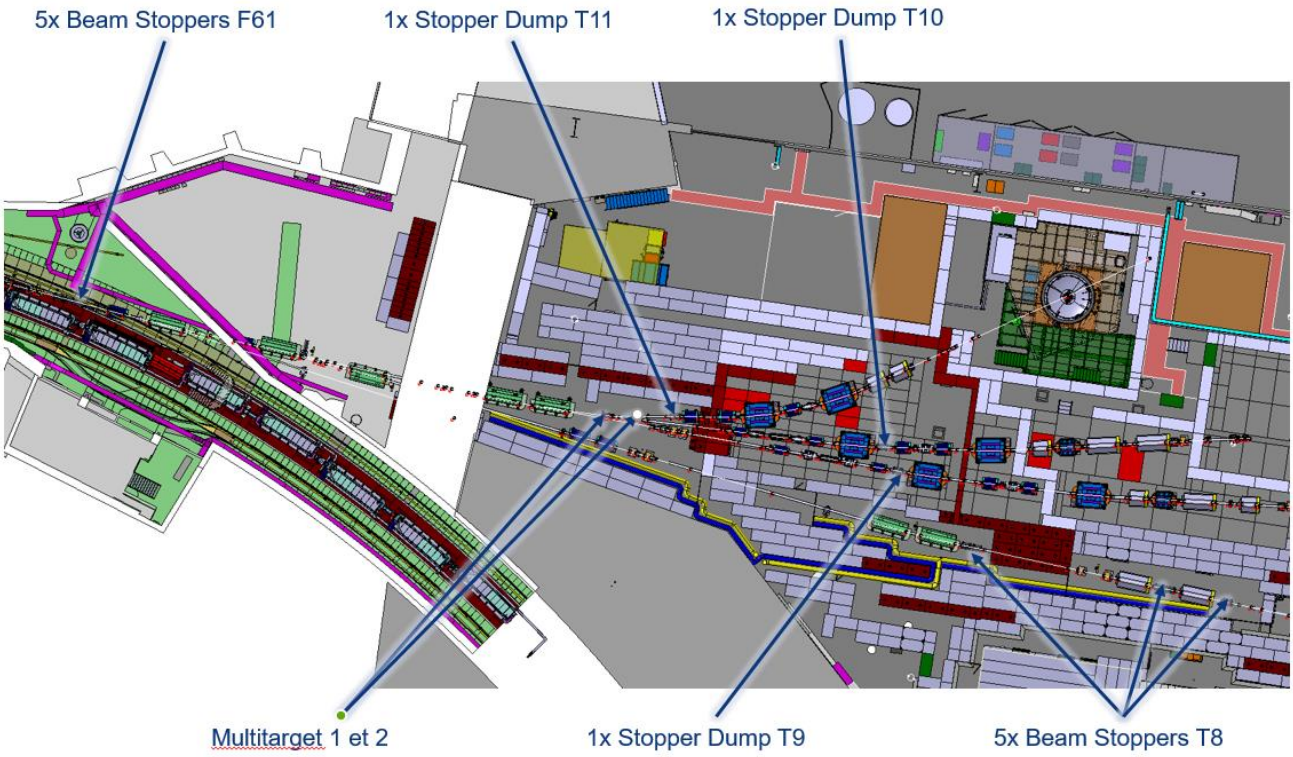

Fig. 4-23: New integration of the beam stoppers, stopper dumps, and multitargets.

4.5 Beam instrumentation

Most of the present beam instrumentation is preserved in the future East Area configuration [46]. The main changes concern their integration into the layout of the new experimental lines. Some old beam profile monitors in the secondary beamlines will be replaced by new ones based on scintillating fibres. New beam loss monitors will be installed along the primary lines F61, T08, and around the two multi-targets. The monitors listed below are classified by main observable.

4.5.1 Intensity measurement and particle counters

The measurement of bunched beam intensity in the transfer lines is performed by fast beam current transformers (BCTF). During slow extraction, where the beam is debunched, the BCTF cannot measure the spill due to the monitor's limited bandwidth (low cut-off frequency), and also due to the low particle flux. Most of the time, beam interacting devices are required in experimental beamlines.

4.5.1.1 Beam current measurement based on gas: BCGAA (formerly named LSD)

The longitudinal spill detection relies on collecting beam-induced ionization photons with nitrogen gas. The electric signal generated by a photo-multiplier (PM) is amplified and sampled. As shown in Fig. 4-24, the plot of the longitudinal spill is displayed on the East Area Vistar for routine check by the operators. Only one device will be kept after the renovation. The monitor's position will be about the same, i.e. 22 m from the extraction point, before F61.MBXHD025 in the new layout (see Table 4-12).

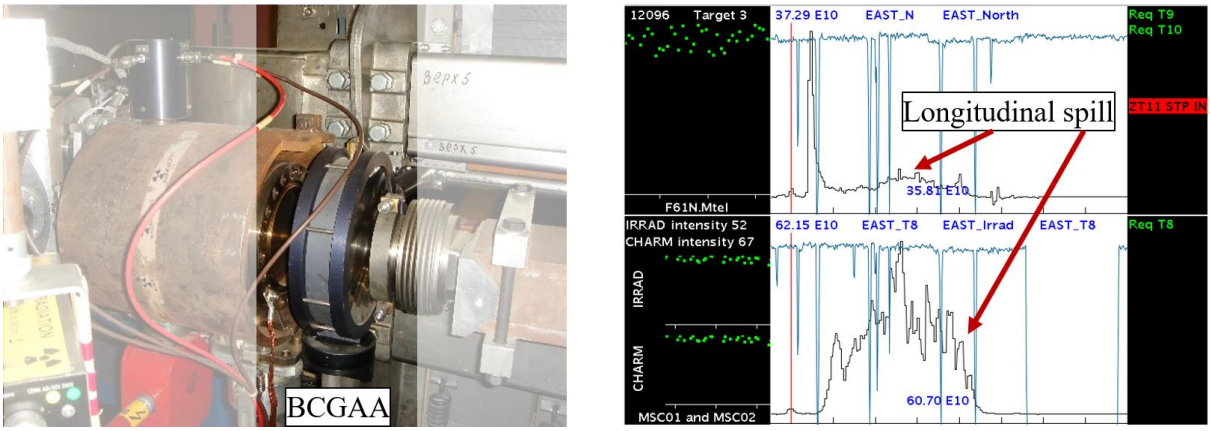

Fig. 4-24: Left: longitudinal spill detector; right: signal from the monitor displayed on EA Vistar.

Table 4-12: Position of BCGAA in the new primary lines.

Line section	Layout component name after LS2	Equipment code
F61	F61.BCGAA023	BCGAA

4.5.1.2 Secondary emission chamber: XSEC / XION

The phenomenon of secondary electron emission from the surfaces of thin metal foils hit by charged particles can be used for particle detection. The so-called secondary emission chambers (XSEC) [44] consist of a stack of plain and polarized hollow thin metal films in vacuum: secondary electrons collected by high voltage electrodes are proportional to the total number of incoming particles. Calibration with a bunched beam (protons or ions) is performed before each run. The comparison of signals from F61.BCTF022 with secondary monitors gives a scaling factor so that the total beam flux and intensity integrated along the spill is deduced.

The argon ionization chambers (XION) use the ionization of argon by particle collisions and collect the electron charge to count primary ion particles. Twenty-one parallel electrodes (5 um aluminium foils) are placed in a stainless steel vessel filled with pure Ar gas slightly above atmospheric pressure: eleven of the electrodes are connected to a local high voltage battery supply, whereas the ten charge collecting foils are connected to the output. The ionization counter works with no avalanche amplification and gives a small but reliable output signal that mirrors the intensity. The analogue signal is sent towards a counter (scaler) in the APRON equipment room and is controlled by a front-end software architecture (FESA) class. The beam intensity is read by controls for the SPS experimental areas (CESAR) system.

Few beam monitors can operate in the target zone due to the very high activation level, but XSEC and XION can withstand high levels of radiation. Both are shown in Fig. 4-25, with the figure of merit for the operators displayed in Vistar (red circles).

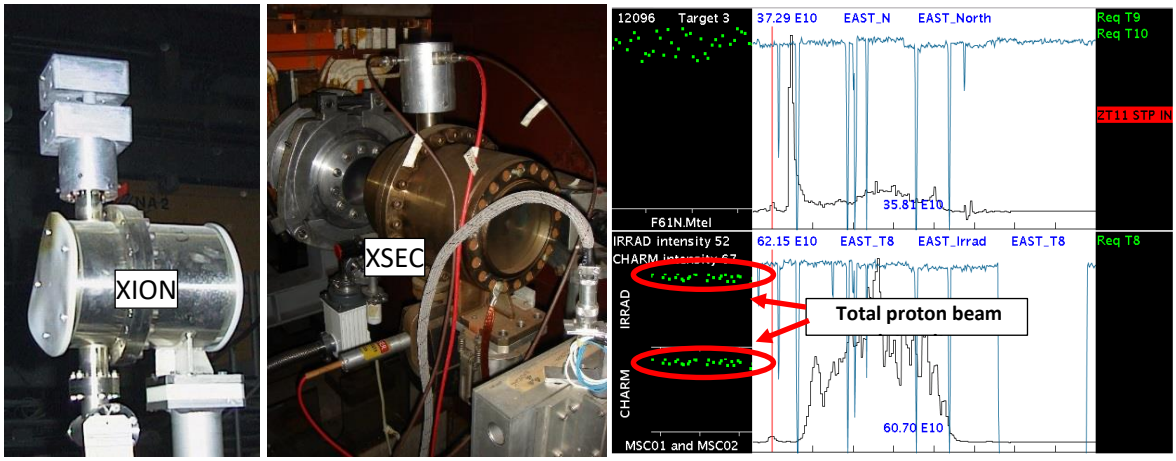

Fig. 4-25: Left: pictures of secondary emission chamber, middle: argon ionization chamber; right: each green dot represents the integrated beam intensity per extraction.

After renovation, all secondary emission chambers will be kept at their current positions in the beamline, except the one in F61, that will be relocated downstream for integration reasons. Like the F62 target, the new target in the F63 line will be equipped with a XSEC. In total, five monitors will be deployed in the new EA layout (see Fig. 4-26). Table 4-13 lists their positions in the extraction line sections and their names in the new layout after renovation.

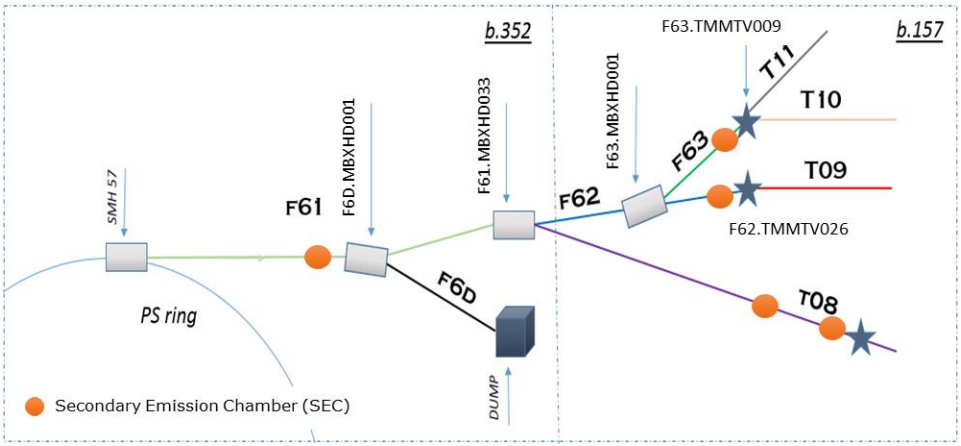

Fig. 4-26: Position of XSEC on the new East Area lines.

Table 4-13: Position of XSEC-XION in the new primary lines.

Line section	Layout component name after LS2	Equipment code	Comment
F61	F61.XSEC023	XSEC	
F62	F62.XSEC022	XSEC	F62 target zone
F63	F63.XSEC008	XSEC	New F63 target zone
T08	T08.XSEC070	XSEC	
T08	T08.XSEC094	XSEC	
T08	T08.XION094	XION	

4.5.1.3 Fast current transformer: BCTF

As mentioned in Section 4.5.1, the monitor F61.BCTF022 is used to calibrate XSEC and XION with bunched beams (see Table 4-14). The current transformer will be kept as it is.

Table 4-14: Position of BCTF in the new primary lines.

Line section	Layout component name after LS2	Equipment code
F61	F61.BCTF022	BCTF

4.5.1.4 Beam loss monitoring (BLM) system

Initially not present in the baseline of the East Area Renovation project, a system to acquire and process the data from 15 BLM detectors spread along the lines has been installed in the East Area, with the scope of observing the beam losses in real time and optimizing the beam process. The new system will be generic and highly configurable. It is based on the ionization chamber (IC) design developed for the LHC that are now widely used in the CERN accelerator complex. Similarly, all the electronics will be of the LHC Injector Upgrade (LIU) type that has recently been deployed for the next run. The technology is reliable, radiation hard, and comes with standard spare parts.

In total, seven BLM detectors will be installed along the primary lines, starting from the PS extraction to the IRRAD and CHARM experimental areas. The beamlines concerned will be F61, F62, F63, and T08 as shown in Fig. 4-27.

Eight additional detectors will be installed in sets of four units downstream of the T09 target (F62.TMMTV026) and the T10/T11 target (F63.TMMTV009) as shown in Fig. 4-28. The idea is to equip each target with a pair of BLMs per plane (horizontal and vertical).

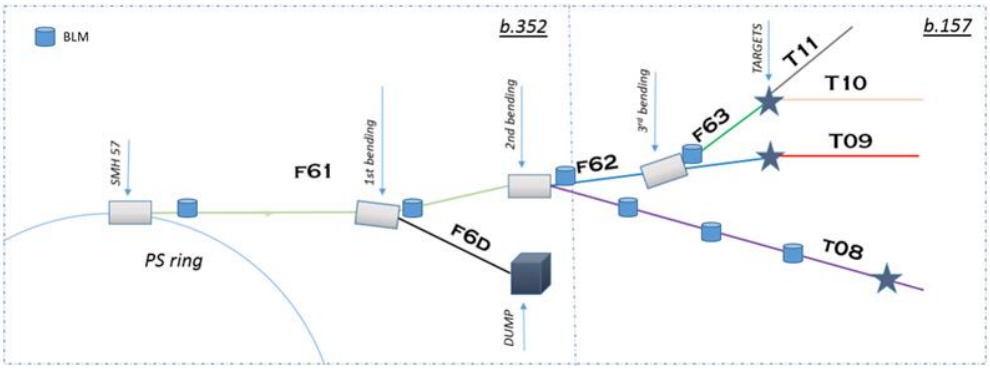

Fig. 4-27: Sketch of BLM detector positions along the primary lines.

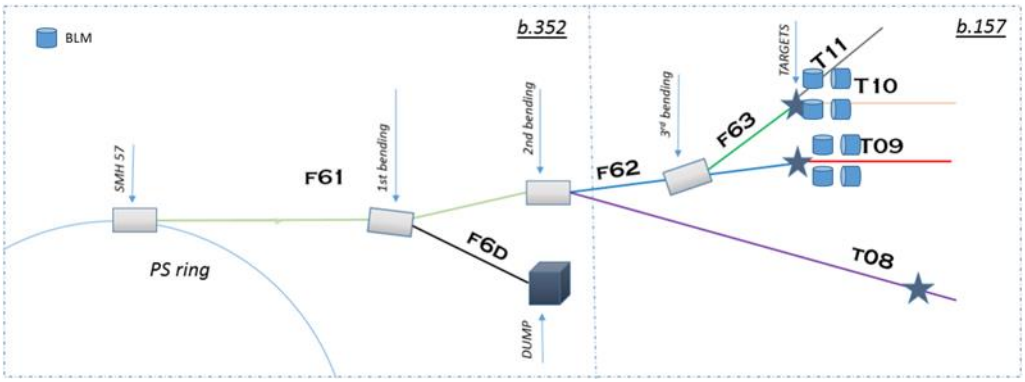

Fig. 4-28: A set of four BLMs will be installed downstream of each target, with the following layout: a couple of units for both H and V planes.

4.5.1.5 Specific particle identification counter based on Cherenkov effect: XCET

Threshold Cherenkov counters are available in some of the East Area beamlines to obtain particle identification information for individual particles in that beamline. The detector is filled with gas that is able to detect particles with speed above the speed of light in the gas. For a certain beam energy, the lighter particles will

have a higher speed. The particles with a speed higher than the speed of light (relativistic particles) inside that particular gas environment will produce Cherenkov light that can be detected by a photomultiplier. The gas pressure inside the detector sets the limit of mass of the particles that can be detected. The beam enters in the detector tube through an entrance window, traverses the tube filled with the selected gas, and exits through the exit window (Fig. 4-29). Inside the top part of the vessel cone, also filled with gas, a mirror deflects the light towards the optical window behind which the photomultiplier is located.

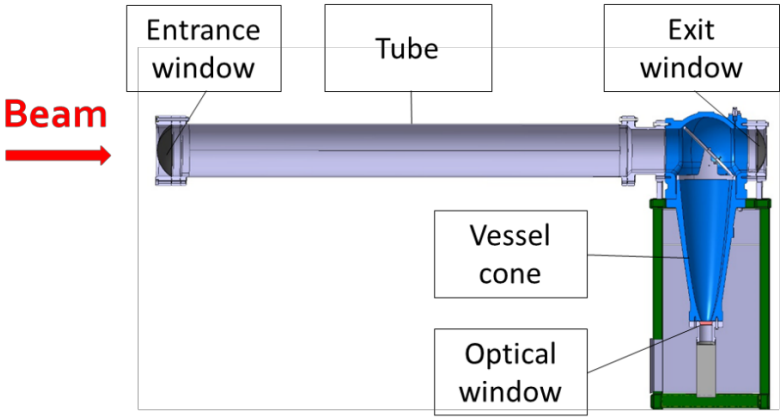

Fig. 4-29: Structure of a Cherenkov counter.

The Cherenkov counters installed in the East Area line consist of a 2.5 m long stainless steel tube with a diameter of 168 mm. The overall desired length should be chosen in accordance with the light efficiency and allowable multiple scattering. Both open ends, the entrance and the exit window of the counter are terminated with 1.4 mm thick aluminium windows. The Cherenkov gases might be selected by the user but should be non-flammable gases, e.g. CO_2, N_2, R218, R134a, etc. to a maximum gauge pressure of 15 bar.

The actual counters are very old instruments, with windows and support structures requiring renovation. Furthermore, the gas pressure is difficult to set precisely and is manually controlled through the old control panel (Fig. 4-32, left). Unlike the North Area, the PM high voltage supply and PM signals are controlled and managed by the users. After renovation, T09 and T10 will be equipped with new pairs of Cherenkov counters. Their respective locations are shown in Fig. 4-30.

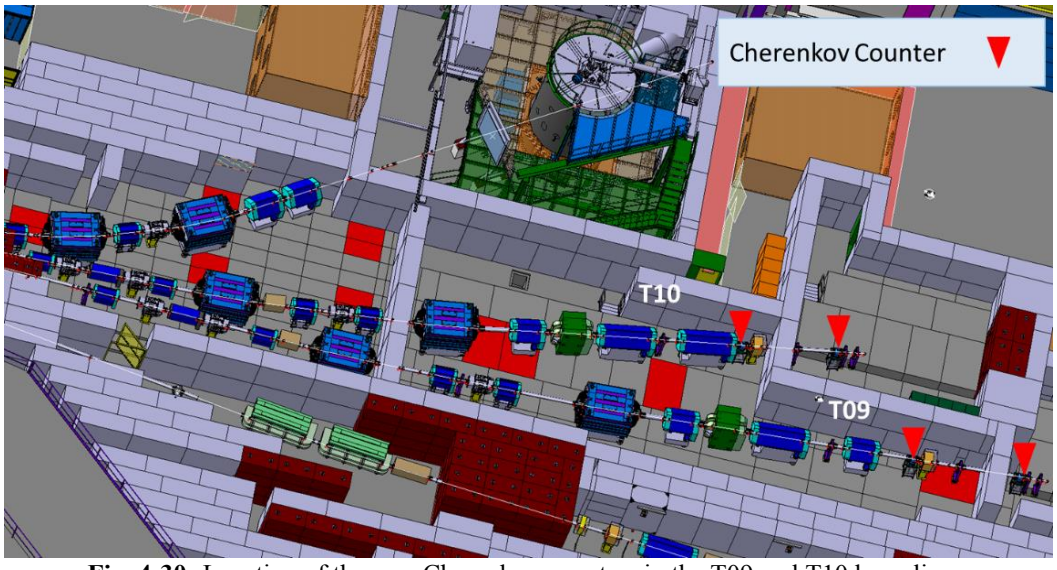

Fig. 4-30: Location of the new Cherenkov counters in the T09 and T10 beamlines.

The structure of the new counters (see Fig. 4-31) is similar to that of Fig. 4-29, with a horizontal tube which can be assembled in a modular way depending on the required length. The latter will be filled with either

N_2 or CO_2 gas under an absolute maximum working gauge pressure of 15 bar. When gas exchange is needed, or the chamber is emptied, the detector remains under primary vacuum. More technical information regarding the new counters is available in Table 4-15.

Fig. 4-31: New Cherenkov counter. Left: body; centre: conical part; right: complete assembly.

Table 4-15: Technical details of the four new Cherenkov counters of the East Area.

Line	Beam aperture (mm)	Total length (mm)	Layout name after LS2	Equipment code
T09	159	3 280	T09.XCET044	XCET
T09	159	3 115	T09.XCET048	XCET
T10	159	2 975	T10.XCET040	XCET
T10	159	2 595	T10.XCET043	XCET

4.5.1.5.1 New acquisition chain and gas control interface

The future acquisition chain will follow North Area standards: the analogue signals are sent towards acquisition modules for Cherenkov counters in the APRON equipment room and controlled by a FESA class. The detector settings will be done by CESAR.

The gas supply line will be updated using a new logic and automation for the gas control system based on low-voltage-controlled valves (Fig. 4-32, right).

Fig. 4-32: Left: actual manual gas control panel for the counters in the East Area. Right: remote control interface for Cherenkov counters in North Area.

4.5.1.6 Scalers

‘Scalers’ are counter channels from a VME board provided to experiments in groups of four. A large experiment can have up to twenty. Scalers are based on SIS3803 modules located in the beam instrumentation (BI) electronic rack in the APRON barrack. A set of four cables per user barrack will be dispatched.

4.5.2 Profile monitors

The beam profile is affected while crossing different accelerator components: bending magnets, quadrupoles, or radio frequency (RF) cavities. A beam width control is important for the transverse matching between machines and also for the beam spot towards the experiments. During slow extraction, profile monitors can serve as position pick-ups. Under such beam conditions, as with the BCTF, standard beam position monitors are blind due to their limited low-frequency bandwidth. There is a large variety of profile monitors, depending on the particle type, current, and energy.

4.5.2.1 Beam observation monitor with fluorescenting screen with scintillating screen and target TV

4.5.2.1.1 BTV with scintillating screen

Following a large upgrade programme undertaken during YETS15-16 to replace the old ‘Marguerites’ stations, proton beam profiles in the PS extraction line F61 upstream of the East Area are now acquired by intercepting the beam with chromium-doped alumina screens and observing the emitted fluorescence with radiation hard cameras. The screen insertion device is made via a vacuum compatible magnetic push–pull system, where bellows are no longer needed. Only the first beam observation monitor with fluorescenting screen (BTV) in T08, which is an operational BTV with bellow (see Fig. 4-33), was not in the scope of the upgrade programme.

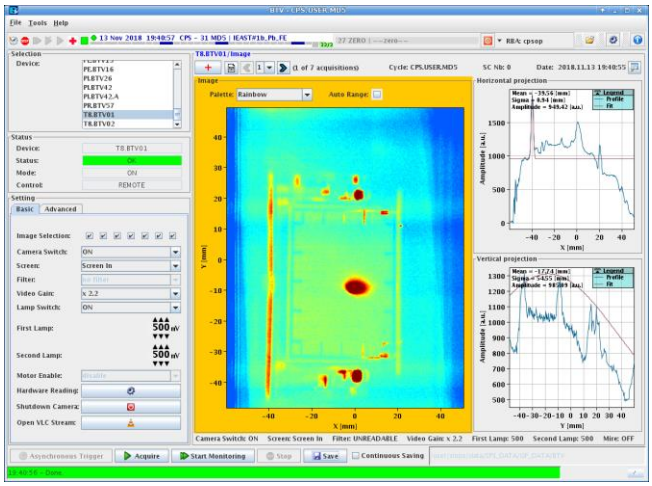

Fig. 4-33: Reference picture from T8.BTV01 during the 2018 ion run.

4.5.2.1.2 Target TV

Besides the secondary emission chamber described earlier, that can operate in a very activated environment, a radiation hard camera is placed upstream of the present F61 target to visualize the beam spot and resteer off-centred beams if needed.

4.5.2.1.3 Layout change during LS2

Only five BTVs out of six will remain in the primary beamlines, with minor changes regarding their positions in the new layout. Currently there are two target TVs, one for the F61 line and one for the CHARM target in the T08 line. After LS2, a third TV will be implemented for the new target in the F63 line. Their positions are schematically represented in Fig. 4-34. Some technical details and new layout names can be found in Table 4-16.

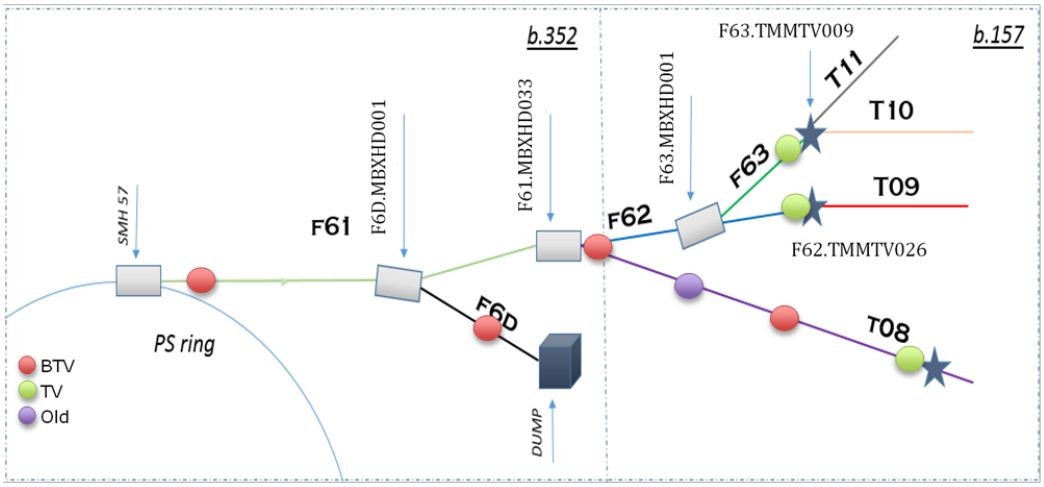

Fig. 4-34: Position of the BTVs in the new layout.

Table 4-16: Technical details and new layout name of BTVs and target TVs after LS2.

Present name	Layout name after LS2	BTV type	Equipment code
F61.BTV01	F61.BTV012	PSZBTVMC (screen 100 mm)	BTV
F61.BTV02	Spare	PSZBTVMC (screen 100 mm)	BTV
F61.BTV03	F62.BTV002	PSZBTVMC (screen 140 mm)	BTV
F61D.BTV01	F6D.BTV010	PSZBTVMC (screen 100 mm)	BTV
F61S.BTV01	T8.BTV020	PSZBTVMC (screen 100 mm)	BTV
ZT8.BTV01	T8.BTV035	Old BTV design, with below	BTV
F61N.BTV01	F62.TMMTV026	Target TV	TMMTV
New	F63.TMMTV009	Target TV	TMMTV
ZT08.BTV02	T08.TMCRT097	Target TV	TMCRT

4.5.2.2 Multi-wire proportional chamber in T08 Line: XWCM

This monitor is mainly used during the commissioning phase of secondary beamlines in the experimental areas. Its typical particle flux range is 10^5 to 10^{11} p/s. The main observables are transverse beam profiles as well as beam position (see Fig. 4-35).

The detector consists of a set of 40 µm stretched tungsten wires, having a 1 mm spacing. The plan is placed between a couple of aluminium foils in a housing containing an equal mix of CO_2 and Ar gas. A high voltage is applied between the foils (cathode) and the wires (anode). The latter collects ionization-induced electrons amplified by avalanche effect. The charges from each wire are integrated during the extraction time. The beam profile is obtained by reading the integrator output voltage from each wire, as shown in Fig. 4-36.

Fig. 4-35: A multi-wire proportional chamber in the North Area (XWCA 021 492).

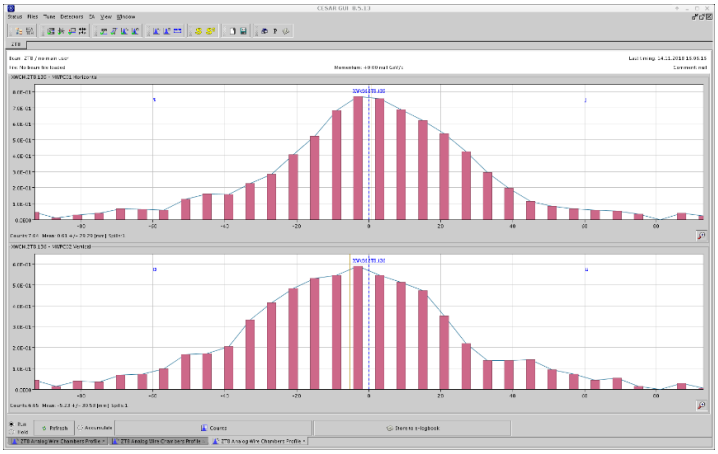

Fig. 4-36: Beam profiles from ZT08.XWCM135 during the 2018 ion run.

This monitor is operational and will be kept without consolidation. Only the layout name will change (see Table 4-17).

Table 4-17: Position of XWCM in the new primary lines.

Line section	Present name	Layout component name after LS2	Equipment code
T08	ZT08.XZCM135	T08.XWCM103	XWCM

4.5.3 Scintillator-based detectors

A scintillator is an organic or inorganic material which emits photons following the excitation of atoms and molecules by radiation (γ or particle radiation including neutrons and neutrinos). The material exists in the three matter phases: solid, liquid, or gas. Scintillators are widely used in secondary beamlines as a multi-purpose monitor, for triggering, or particle identification by pulse height analysis. Other possible applications are light guide, wavelength shifter, calorimeters, or time of flight counters thanks to their very fast response time.

4.5.3.1 Particles counters and triggers: XSCI

Plastic scintillators are currently installed in the East Area as particle counters or triggers. T09 is equipped with a pair of scintillators, while T10 and T11 have only one. PMs with high voltage for light amplification and output signal are connected to a dedicated acquisition module in the APRON equipment room, and controlled by a FESA class. The present detectors are kept, with minor displacement in the new layout. T10 will get a second detector. Their positions and new layout name are listed in Table 4-18.

Table 4-18: Position of XSCI in the new primary lines.

Line	Layout name after LS2	Equipment code
T09	T09. XSCI041	XSCI
T09	T09. XSCI050	XSCI
T10	T10. XSCI036	XSCI
T10, new	T10. XSCI044	XSCI
T11	T11. XSCI022	XSCI

4.5.3.2 Scintillating fibre monitors: XBPF

The experimental beam profile fibre monitor (XBPF) [45] is a scintillating fibre detector recently developed at CERN for the measurement of the profile, position, and intensity of secondary beams. The physics principle of particle detection with scintillating fibres relies in the creation of scintillation light, due to the passage of a charged particle, and the transmission of this light inside the fibre by total internal reflexion. The XBPF is

composed of 100 or 200 scintillating fibres (depending on the size of the monitor) of 1mm thickness and square cross-section. The fibres are packed together along one plane, forming the active area of the detector that stands in front of the beam (Fig. 4-37, left). The light from every fibre is read out on one end by an individual silicon photomultiplier that allows one to know which fibre has been activated and to subsequently measure the profile, position, and intensity of the beam. A mirror glued on the non-read-out end of the fibre reflects back the light travelling in that direction along the fibre, thus increasing the total light signal reaching the photomultiplier.

The XBPF has been designed to be vacuum compatible, which removes the need for vacuum windows, therefore helping to reduce the material budget of the beamline. The photodetectors are located outside vacuum, with the fibres exiting via a feedthrough based on an innovative gluing technique that guarantees the necessary leak tightness. The vacuum tank of the new detectors has a modular design that allows two XBPF to be hosted for the simultaneous measurement of the horizontal and vertical profiles of the beam (Fig. 4-37, right).

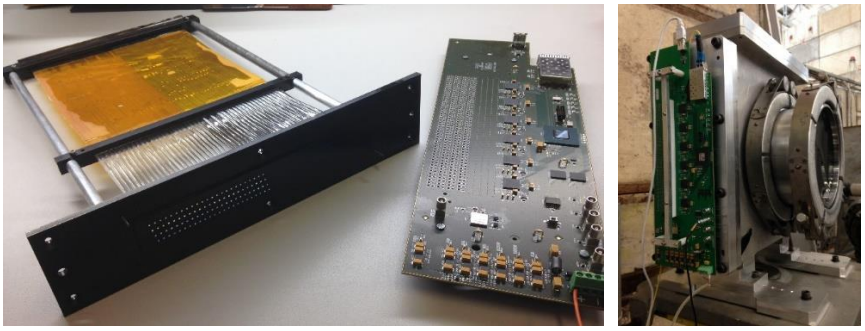

Fig. 4-37: Left: XBPF on the left and front-end board with the 192 SiPMs on the right. Right: vacuum tank of the XBPF during installation, with a front-end electronics board in place.

4.5.3.2.1 New detectors after LS2

These three aging gaseous wire chambers (XDWC) in each of the secondary beamlines, which can no longer provide accurate profiles in all ranges of intensities, will be upgraded by dual-plane scintillator fibre monitors. Table 4-19 summarizes the changes and the new layout names.

Table 4-19: Upgrade of beam profile monitors after LS2.

Line	Changes after LS2	Equipment code	Comment
ZT09	Removed	XDWC	Storage
ZT10	Removed	XDWC	Storage
ZT11	Removed	XDWC	Storage
T09	T09.XBPF041	XBPF	New, 10 cm × 10 cm
T09	T09.XBPF050	XBPF	New, 10 cm × 10 cm
T10	T10.XBPF045	XBPF	New, 10 cm × 10 cm
T11	T11.XBPF022	XBPF	New, 20 cm × 20 cm

To keep the versatility of the new experimental lines, the XBPF tanks will not be pumped down, but left under atmospheric pressure.

4.5.3.2.2 Acquisition chain and cabling

The Beam Instrumentation (BI) group will produce the front-end boards (one per plane). On the back-end side, a VFC-based acquisition board developed by BI for its applications will be used. The transmission between them is performed via optical fibres.

4.6 Survey systems

Due to beam optics requirements, the correct positioning and alignment of all beamline components is mandatory. The future configuration of the East Area will follow the survey requirements in terms of layout [46][47] but also the CERN standards in terms of alignment.

All buildings where the new beamlines will be installed were scanned in three dimensions to do a comparison with the integration model. A difference of 30 mm was found between the PS floor and the East Area Building 157 floor. This height difference will be compensated in Building 157 with the beam equipment supports.

4.6.1 Networks

Before the alignment of the components, a reference network of precise points will be done all around the areas. The positions of these points will be uploaded on the survey database and will be used later to align the equipment.

The network area includes Building 352 and all the beam areas in Building 157 as shown in Fig. 4-38. In order to establish the point network between Buildings 352 and 157 there will be a hole in the separation wall between these buildings. The same procedure must be applied for all internal walls of Building 157 between the closed zones. The network needs to be determined before dismantling the main components already installed in the East Area.

Fig. 4-38: Building 352 (in blue), primary area (red), mixed area (green), T8 area (orange), secondary beam area (purple).

4.6.2 Fiducialization

Each component to be aligned will have two survey fiducials (usually spheres) on top of it, indicating the entry and exit of the element ('Entrée+Sortie' E + S) plus a tilt surface to measure the angle of the element. The two fiducials installed on the components should leave enough space to put the measuring system on top (min. 50 cm).

In order to align each component with respect to the network, a fiducialization step has to be performed before installation. The fiducialization is a procedure where the relative positioning between the two survey fiducials (E+S) is measured with respect to the theoretical beam axis of the component. The fiducialization is a procedure done before installation. The values coming from the fiducialization step give the geometry of the

component. These values are saved in the Geode database and the CERN Coordinate System (CCS) is calculated for each component.

4.6.3 Ground marking

Once the network is installed in the area, the ground marking of the theoretical beam axis is done. The beamline is calculated starting from a MADX file of the beamline. The line is also inserted in the database Geode. For each component, the E + S references will be also marked on the ground. The theoretical beamline serves as a reference also for others services (cabling, handling, cooling and ventilation, support installation, transport).

4.6.4 Alignment

Once the fiducialization for the components and the ground marking is done, the installation and alignment of the beamline equipment can then be done. The network is used as reference for the measurements and the alignment is done following the beamline optic coming from the methodical accelerator design (MADX) file saved in Geode. There are two steps of alignment: the first consists in the alignment of the supports and the second is the alignment of the components. Depending on the type of support and the components used, the alignment methodology is different.

The standard supports are positioned according to the ground marking. The adjusting table of the support is regulated up to the desired position and then the component is placed on top. The survey fiducials on each component are measured using a laser tracker and an optical level; also the roll angle is measured using an inclinometer. The position of the components is cross-checked on the database.

In the primary area, beamline components will be installed on plug-in supports, which will suppress the need for alignment intervention in the future to reduce the exposition of surveyors to ionizing radiations. For this area, the fiducials are directly installed on the supports that are aligned following the standard procedure. The beamline components will be prepared outside the primary area and the final alignment will be ensured by the plug-in system (based on metallic jacks) without further need for intervention.

4.6.5 Smoothing

The smoothing is the final step of the alignment procedure and is usually done just before beam commissioning. All components are measured in the vertical and radial directions and the data are used to create a smoothing beam curve. All components should be on the curve; if a component is out of the tolerances, it will be realigned.

4.7 Machine interlocks

4.7.1 Introduction

The interlock systems constitute a vital part of the machine protection systems and protect the different machine elements from damage. In the case of the East Area, a machine interlock system for the protection of the resistive magnets is in place. Under the mandate of the EA Renovation project, it was decided to replace this legacy interlock system, as part of the renovation of the magnets, with a standardized warm magnet interlock controller (WIC) system. As a generic solution to the interlocking requirements existing throughout the CERN complex, the functionality of the WIC system for the East Area will be identical to the other WIC systems already in operation in the CERN Accelerator Complex or other experimental areas (e.g. Elena). No other machine interlock systems will be installed in the East Area and for this reason, no equipment will be able to automatically stop the beams by hardware.

4.7.2 Warm magnet interlock controller system

4.7.2.1 Warm magnet interlock controller system overview

The warm magnet interlock controller (WIC) system is in charge of protecting the resistive magnets against overheating [48]. It is a PLC-based system. The central processing unit (CPU) of the PLC is the central controller and, in case of overheating of one of the magnets protected, will send the fast abort signal to the corresponding power converter that powers the magnet. The temperature of the magnets is compared against a pre-set limit by several thermo-switches installed on the magnet coils or busbars and the flow of the cooling system of the magnets is also monitored by the WIC. In the case that abnormal conditions are detected, the WIC will react to protect the magnets. A schematic figure depicting the WIC system can be found in Fig. 4-39.

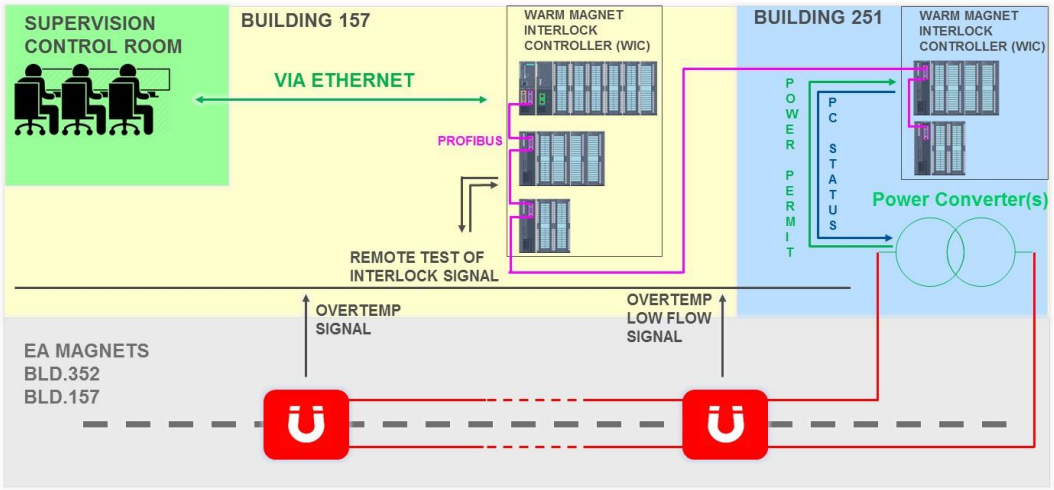

Fig. 4-39: Simplified layout of the WIC system for the East Area.

The WIC system is highly reliable and assures the minimum downtime due to failures of the protection system. The system was designed as a standard solution to be deployed CERN-wide. In the case of the East Area, there is no link to the beam interlock system.

The WIC uses a generic software program and a homogeneous hardware solution to adapt the specific interlock requirements to the existing layout. The layout is described within a database (including magnet names, input and output addresses, power converters, interface types, and others). The specific information for each installation is extracted in different configuration files that will be used to define the system in accordance with the project requirements.

4.7.2.2 The WIC layout for the EA

The dedicated WIC to protect the 58 magnets located along the F61 line, in the primary and secondary areas of the EA will be installed during LS2. The system will have two dedicated racks (Fig. 4-40), one for the control and the acquisition of the magnet signals located in the Apron room (157/1-009), and another located in Building 251 to control the 61 power converters. The details of the WIC configuration of the EA can be found in Ref. [49].

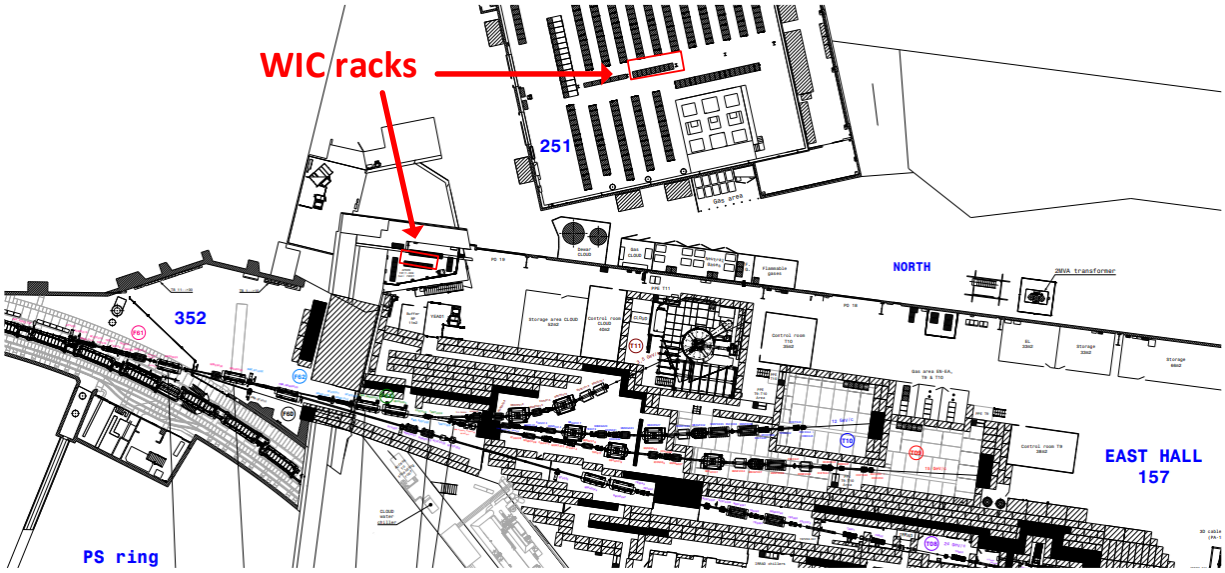

Fig. 4-40: Layout of the East Area with the location of the two WIC racks.

4.8 Beam controls

4.8.1 Upgrade of the infrastructure

The control infrastructure provided by the Controls Group (BE-CO), Beams Department, will be upgraded for the EA as part of the overall initiative to upgrade the hardware and software components during the long shutdown LS2. New pulse repeaters (for the distribution of pulses) and new a general master timing (GMT) distribution to all front-end computers (FECs) will be installed as well as new hardware components, replacing the ageing components dating from 1980 with enhanced remote monitoring and diagnostics of the whole distribution chain. New full digital distribution system (Matrox digital decoders) will replace the old analogue video distribution system (CATV) (Fig. 4-41).

All FECs used in the East Area had to be upgraded to FESA3 version 7 and to CENT-OS7 by 1 January 2020; this date corresponds to the official end of life milestone for all BE-CO legacy components [50]. The upgrade is under the responsibility of persons in charge of the FEC and of the FESA classes.

Fig. 4-41: New video distribution system.

4.9 Collimators

4.9.1 General description

The collimators are devices composed of internal jaws that are moved according to the operation requirements to clean the beam by removing stray particles and protecting downstream equipment, shielding it from beam trajectory errors. The internal aperture of a collimator can be used to define the range of beam energy, reduce the beam intensity (acceptance collimator), find the beam by scanning the aperture, divide particles of different types, and clean the beam disturbed by other collimators upstream.

The T09, T10, and T11 secondary beamlines are equipped with obsolete PS-type collimators, poorly documented for their mechanics and with replacement parts hard to find. In addition, the current collimators are also incompatible with computer control. Mechanical failure is the main issue with the beamline collimators such as jammed positioning mechanism, broken ribbon, or faulty ball bearings or potentiometer. Electrical failure is also likely including motor fault, impossible data reading, problems with electronics given by the high radioactive environment, etc.

It is therefore proposed to replace the old East Area collimators by four 4-jaw collimators (XCHV) taken from the North Area spare collimators [51] and three new 2-jaw collimators (XCSV and XCSH). The spare collimators of the North Area can be re-used provided that a thorough refurbishment is completed and validated by commissioning tests. The new collimators control system will be done via FESA classes, logged and controlled by CESAR and TIMBER.

By using XCHV and XCSV/H, collimators already used in the North Area it will be possible to make the device types and controls used at CERN in the experimental areas more uniform, easing the standardization and classification of equipment and control systems.

In total, 7 new collimators will be installed: 3 XCHV for T09, 1 XCHV, 1 XCSH, and 1 XCSV for T10 and 1 XCSH for T11 (see Fig. 4-42). In addition to these collimators, a new fixed collimator, the XTCX, will be added at the beginning of the T09 line during LS2 (see Section 4.9.4).

Fig. 4-42: Location of the new collimators in T09, T10 and T11.

4.9.2 XCHV collimator design

The XCHV collimators have four internal jaws made of steel (in grey in Fig. 4-43) of which two are moved along the horizontal direction and two along the vertical one. Every jaw is motorized and the position is controlled by a linear potentiometer (Fig. 4-44).

The external structure of the collimator is a vacuum vessel that is connected upstream and downstream with the vacuum beam chamber.

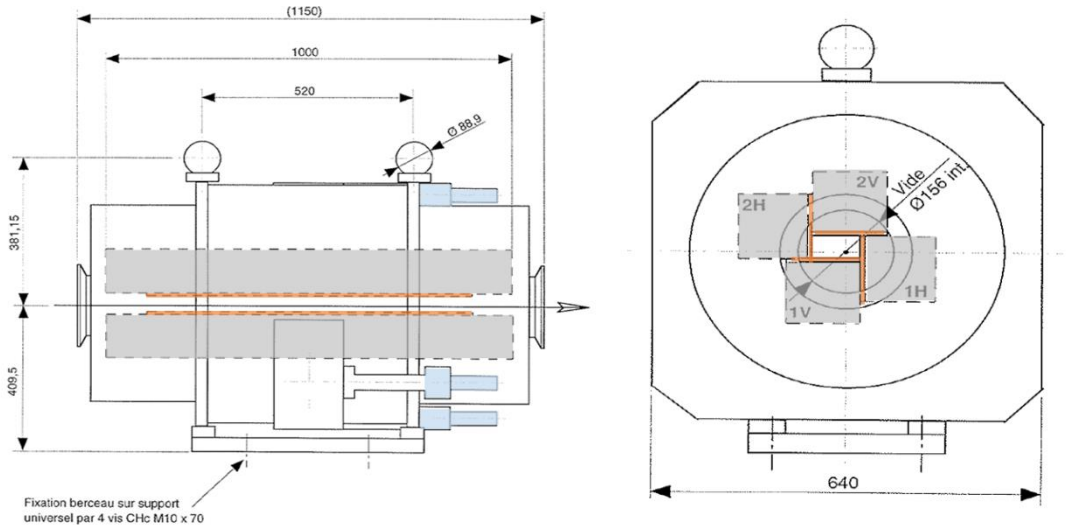

Fig. 4-43: XCHV collimator drawing a longitudinal view and upstream view of the open collimators with jaws.

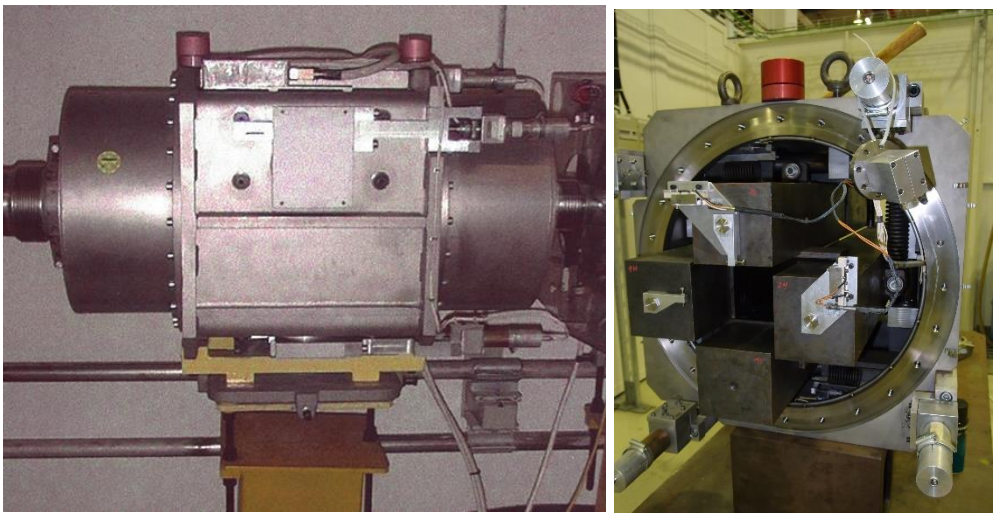

Fig. 4-44: Longitudinal view and downstream view of an open collimator with the jaws and motors.

4.9.3 XCSV-XCSH collimator design

The XCSV and XCSH collimators (Fig. 4-45) have two internal steel jaws that are able to move horizontally (XCSH) or vertically (XCSV) driven by a DC motor and their position is controlled by a linear potentiometer. Each jaw is moved by a motor operating in DC. Two micro-switches are mounted externally to indicate the end of the outer movement and a third micro-switch is installed internally in common with the two jaws to avoid collisions between them.

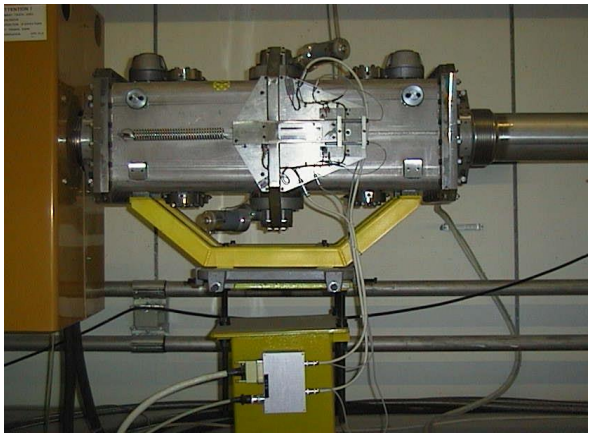

Fig. 4-45: Longitudinal view of a XCSV or XCSH collimator.

4.9.4 XTCX collimator

The XTCX (TCX stands for 'target collimator experimental areas') is a beam collimator that serves to protect the facilities placed after the target [51]. It is designed to withstand primary beam intensities. It is composed of an iron block mounted on an aluminium frame. The iron block permit absorption of the beam with a variable momentum spread in order to transmit only the wanted secondary beam with a specific central momentum. The XTCX is located on T09, just after the target (Fig. 4-46). No vacuum chambers pass through the XTCX. The beam passes through the air and comes back through a vacuum chamber just after the XTCX, passing through a 0.1 mm thick aluminium window. It is a passive component without water cooling. Design details can be found in Refs. [52] and [53].

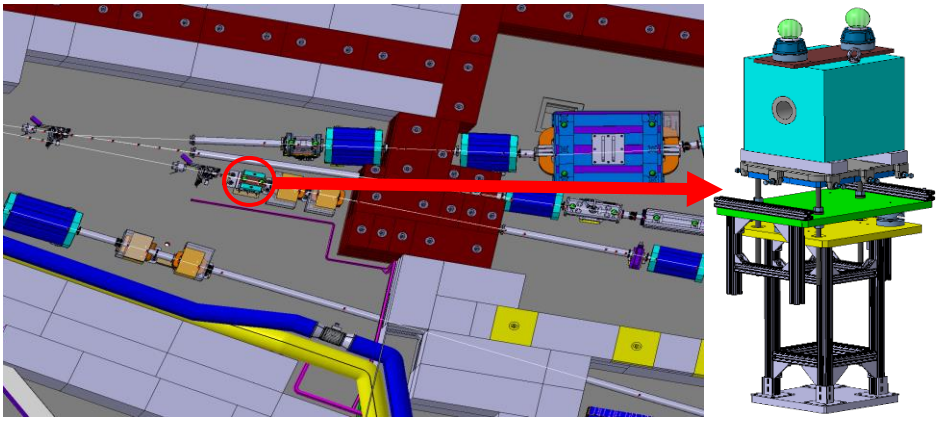

Fig. 4-46: Location of the XTCX in the T09 line.

4.10 Radiation shielding

4.10.1 Facility parameters

The beam parameters that were used for the design of the shielding were taken from Ref. [54]. The East Hall receives a slowly extracted proton beam from the CERN PS with a beam momentum of 24 GeV/c with up to 5×10^{11} protons per pulse and a maximum average beam intensity of 6.7×10^{10} protons per second. Theoretically, up to 6 spills per supercycle of 45.6 seconds can be sent to the East Hall, up to 3 spills per supercycle for T09, and up to 3 spills per supercycle for T10, with 3.3×10^{10} protons per second for each target.

Accounting for the number of days of operation per year and machine availability, the nominal annual number of protons is 3.3×10^{17} protons per year and the maximum annual number of protons is 10^{18} protons per year.

4.10.2 Radiation protection requirements

The shielding of the East Area primary zone has to be designed so that the radiological area classification [55] for the East Hall is respected. Being classified as a Supervised Radiation Area, this means that the ambient dose equivalent rates should be below 3 μSv/h for the control rooms inside the East Hall and less than 15 μSv/h (low occupancy area) at 40 cm outside the shielding walls for the maximum average beam intensity of 6.7×10^{10} p/s, at locations accessible during beam operation. In addition, the ambient dose equivalent rates should be below 2.5 μSv/h outside of the hall for the maximum average beam intensity. These requirements mean that all shielding passages (access chicanes, ventilation ducts, cable ducts) have to be designed in an optimized way.

In addition to compliance with the limits of the radiological area classification, the shielding has to be designed so that the ambient dose equivalent rates are well below the corresponding radiological area classification limits at the most important locations, e.g. the control rooms, for optimization reasons. The shielding also has to be designed so that the annual effective dose to the members of public, combined from prompt radiation (sky shine) and from releases to the environment, is less than 1 μSv for the nominal annual number of protons on the targets.

The design of the shielding tries to make use of as many existing concrete and iron shielding blocks as possible. The design has to take into account the fact that there is limited space due to the already existing facilities in the rest of the East Hall. Monte Carlo simulations were performed with the FLUKA [56][57] code to estimate the prompt ambient equivalent dose rate levels for East Area Primary Zone.

4.10.3 PS - primary ring zone

The shielding in the PS extraction towards the East Area Primary Zone, was placed to protect persons in the Primary Zone during accesses from beam losses in the PS. Three loss point locations have been studied for two beam loss scenarios.

The first loss scenario is a continuous loss in the PS. After discussion with the Operation Group (BE-OP), a 3% loss of all beams injected in the PS was taken into consideration. Being driven mainly by the SFTPRO beam, 4 cycles per supercycle with 2×10^{13} protons per cycles for the SFTPRO beam have been assumed. In order to estimate the continuous loss close to the PS extraction towards the East Area Primary Zone, this intensity was scaled with the ratio of the sum of the residual dose rates in PS sections 61 to 71 compared to the sum of the residual dose rates in the full PS ring based on radioprotection (RP) survey data. The resulting continuous loss rate was rounded up to 5×10^{9} protons per second.

The second loss scenario was to take into account the full beam loss of one SFTPRO cycle, i.e. 2×10^{13} protons.

The simulation results for the 3 loss point locations were normalized with these two loss scenarios and the ambient dose equivalent rates and ambient dose equivalent were investigated to design the shielding around the F61 beamline leading to the East Hall and to implement it accordingly [58]. The final design of the shielding, after the above mentioned studies, around the F61 beamline can be found in Fig. 4-47. The ratio between the dose rate at the location of the dose monitor PAXP502 (entrance of Building 352) and the dose rate at the beginning of the Primary Zone will be used to ensure proper area monitoring of the Primary Zone by adapting the dose rate alarm threshold of PAXP502 if needed.

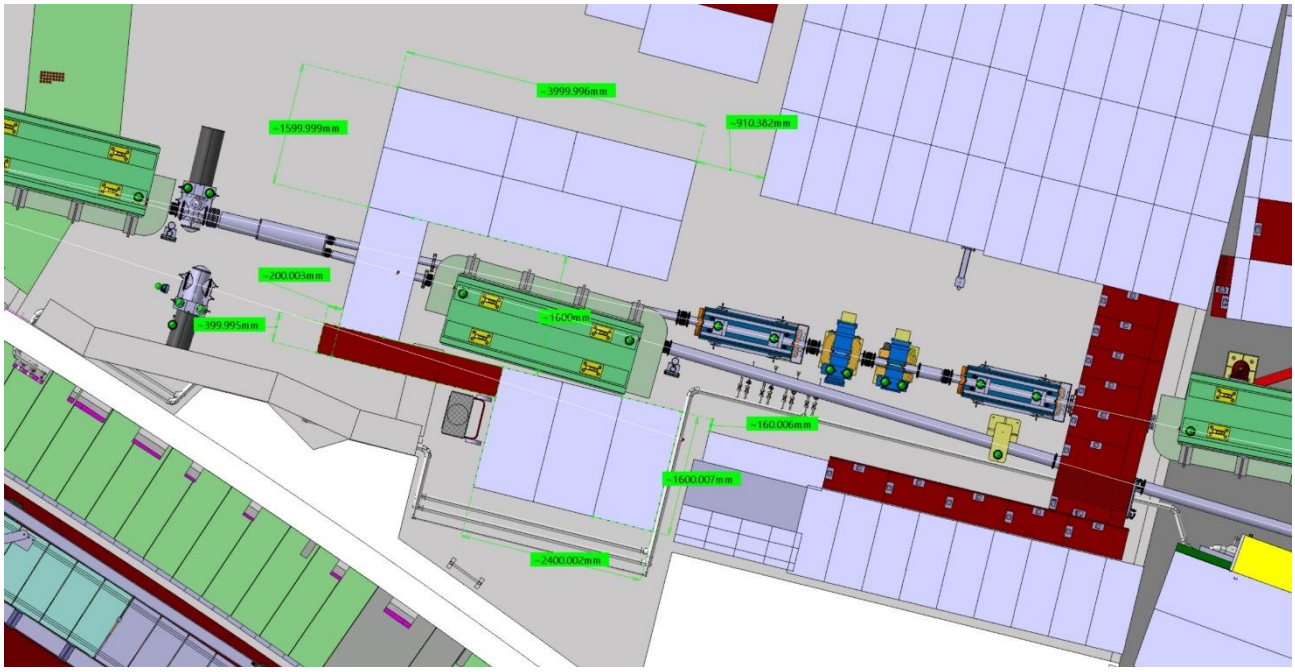

Fig. 4-47: PS – Primary Zone, in CATIA model.

4.10.4 The Primary Zone

Simulations [59] have been performed with the FLUKA code for the shielding of the Primary Zone. The shielding is presented in Fig. 4-48. The design of the access chicane towards the primary zone was based on the simulation studies as well as the shielding towards the access point on the south side.

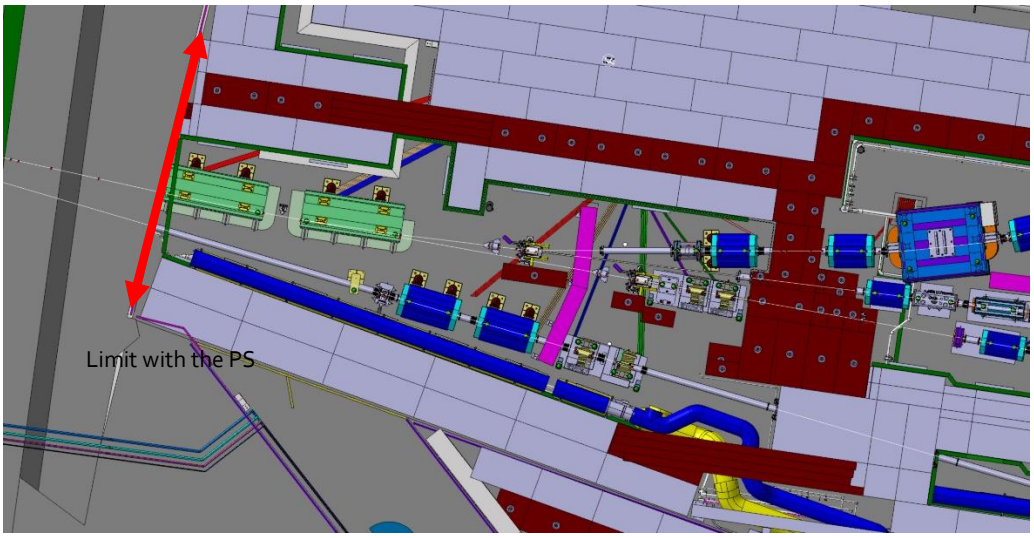

Fig. 4-48: Top view of the primary without the roof.

The shielding of the roof above the Primary Zone starts at 3.2 m height of the Primary Zone room and consists of 0.8 m of concrete, 0.8 m of cast iron, and 3.2 m of concrete (up to 8 m from the floor level). The roof shielding covers all of the Primary Zone area and continues until the access doors (Fig. 4-49). The optimization of the shielding on the edges will be based on the simulations by FLUKA.

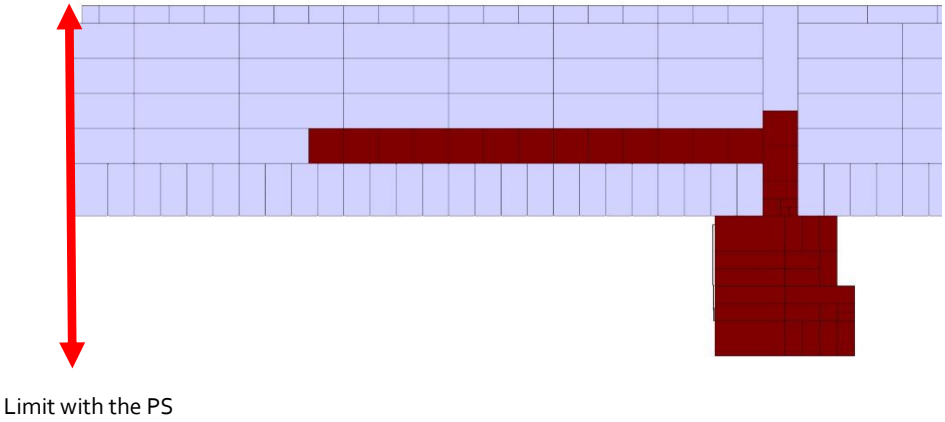

Fig. 4-49: Vertical cut of the primary area roof.

4.10.5 Beam dump for the F62 and F63 beamlines

The beam dump design is very important because it affects the prompt and residual radiation values upstream and downstream of it.

Several scenarios were studied for the dump between the Primary Zone and the mixed zone, taking into account the prompt and residual radiation. The dump optimization has yielded a significant reduction of the prompt dose rate downstream and on the roof, leading to a reduction of shielding thicknesses. The most suitable dump configuration was chosen, taking into consideration the construction, radiation, and cost constraints. The optimized configuration of the dump is shown in Fig. 4-50, with a tungsten block of 20 cm × 20 cm × 40 cm at the T10 line, see Fig. 4-51, inserted in the dump 10 cm downstream of the front face of the dump and centred around the beam. The additional shielding for the T09 beam dump is shown in Fig. 4-52.

The residual dose rate optimization in the primary zone will be done by installing a movable shielding, mounted on rails, to cover the two impact points of the beams T09 and T10 on the dumps and centred around the beam, during accesses.

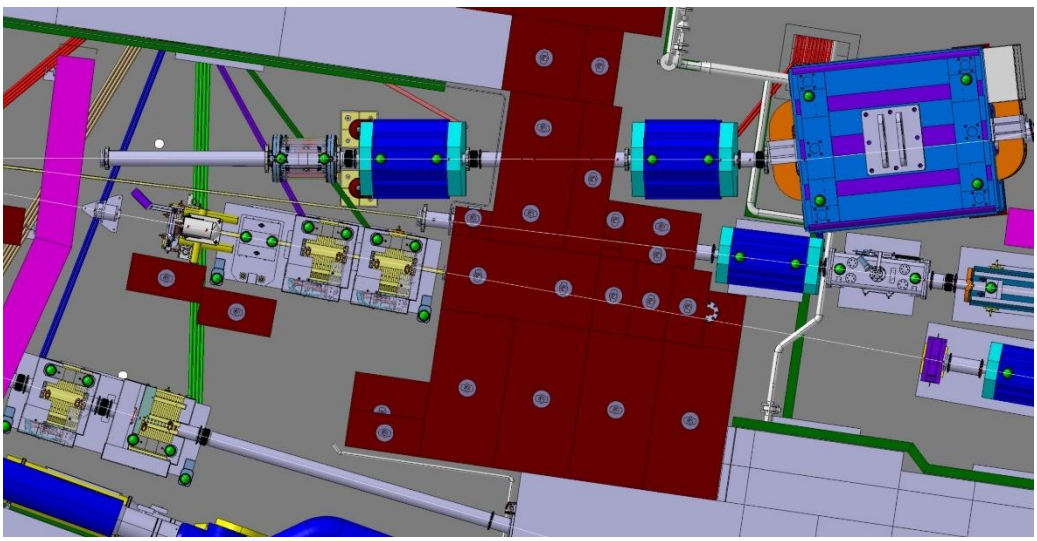

Fig. 4-50: Optimized configuration of the dump in CATIA model.

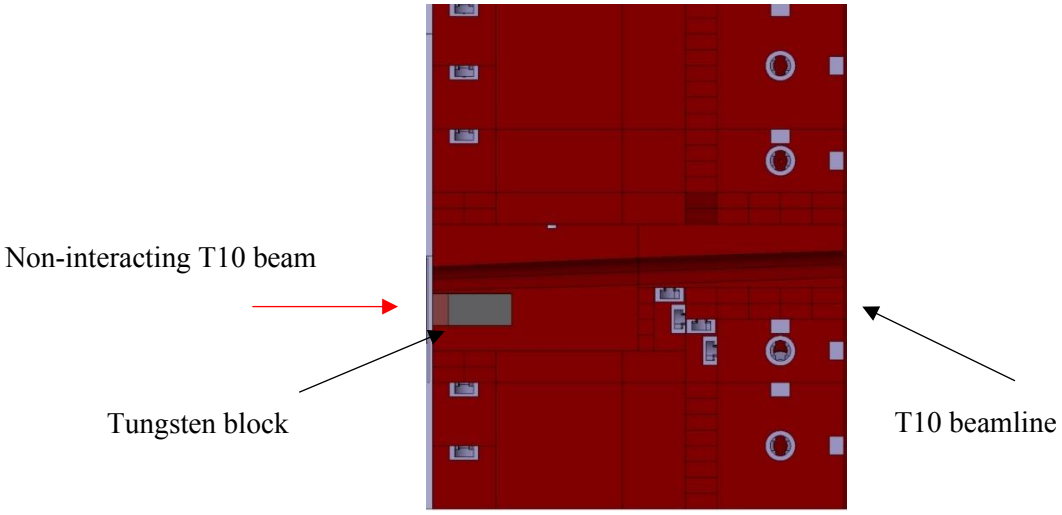

Fig. 4-51: Tungsten block of 20 cm × 20 cm × 40 cm at T10 beamline.

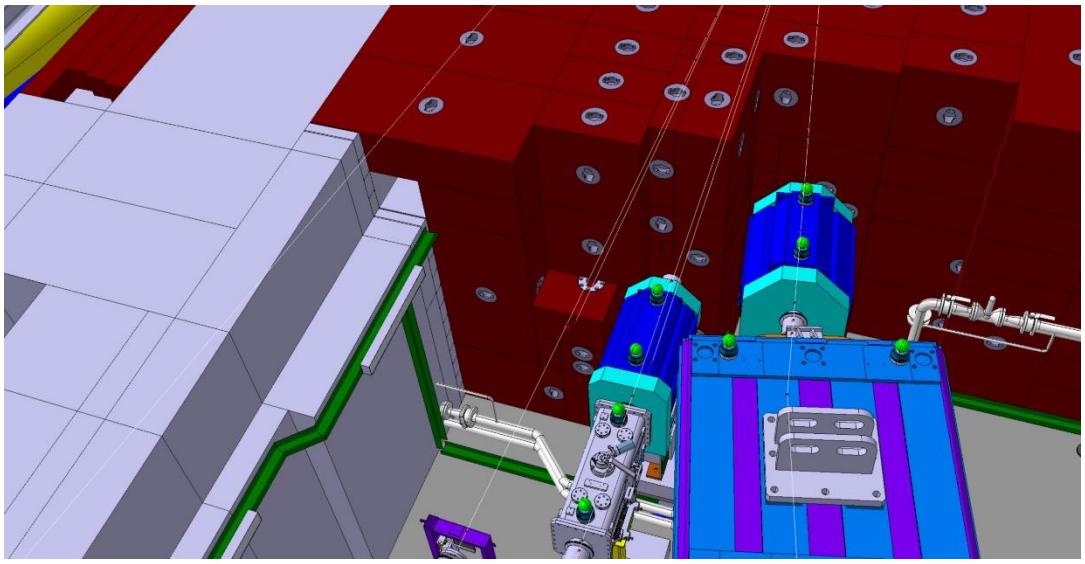

Fig. 4-52: T09 side of the beam dump.

4.10.6 Mixed zone

The shielding of the mixed zone, see Fig. 4-53, was designed taking into account the radiation derived from the dump and the beam losses of the secondary beams transported in T09, T10, and T11.

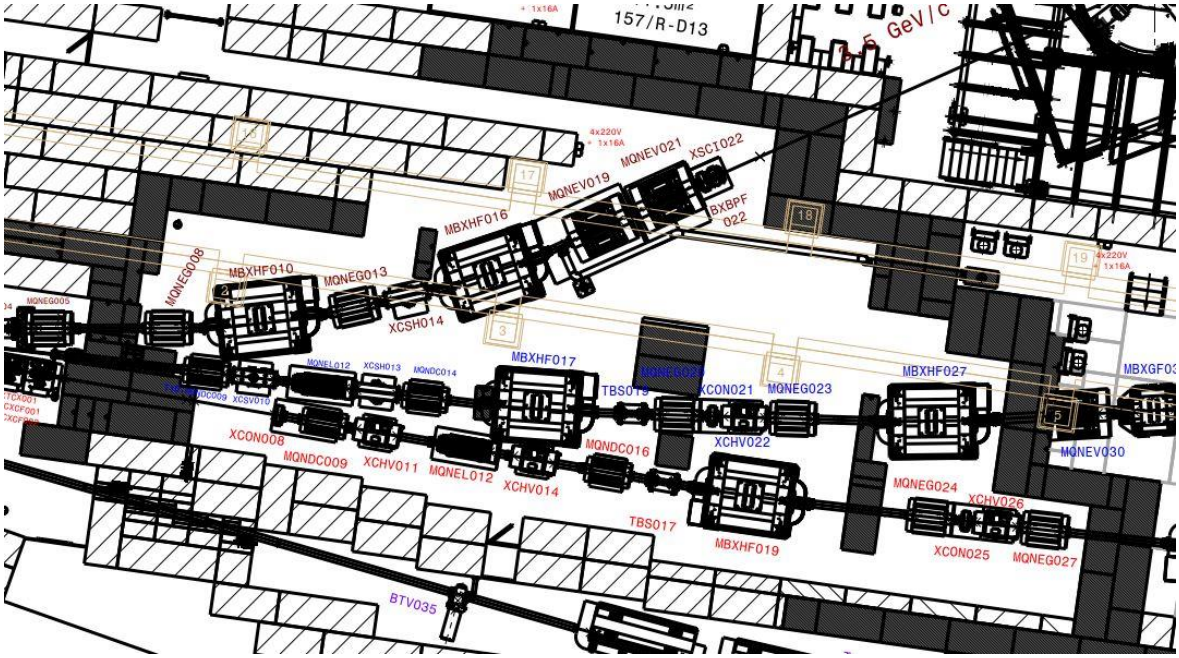

Fig. 4-53: Mixed zone.

The shielding of the roof above the mixed zone has been defined by FLUKA simulations. It starts at a 3.2 m height of the mixed zone and consists of a 3.2 m to 4.4 m height of concrete shielding (Fig. 4-54).

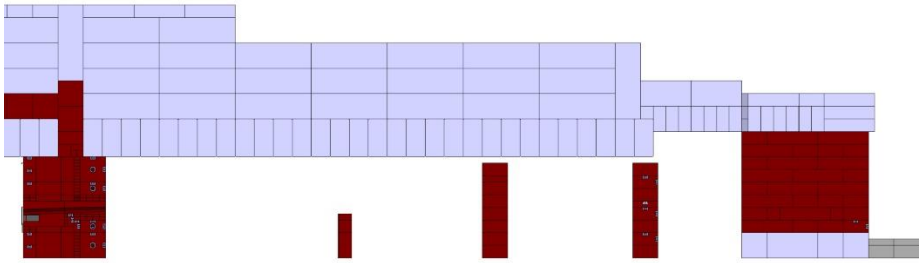

Fig. 4-54: Vertical cut of the roof shielding at the mixed zone.

4.10.7 T09-10 zone

For the T09 zone, the T09 experimental zone beam dump was designed taking into account a pion beam of 15 GeV/c with a maximum 5×10^6 pions per spill. The shielding in Fig. 4-55 shows that the T09 control room is not in direct continuation of the T09 beamline, in order to avoid the direct muons coming from the beam traversing the shielding.

Fig. 4-55: T09-10 experimental zone.

4.11 Radiation monitoring

4.11.1 Purpose of the radiation monitoring system

The purpose of the radiation monitoring system is threefold. First, it has to provide radiological area surveillance to ensure that the ambient dose equivalent rates at locations accessible during beam operation remain below the limits determined by the radiological area classification. Second, the radiation levels due to residual radiation are measured prior to granting access to the primary zone to ensure that the radiation levels are optimized and that they are consistent with the ones used for the work and dose planning. Third, the airborne radioactivity that is released by the ventilation system to ensure the dynamic confinement of the primary zone is monitored.

4.11.2 Radiation fields in the East Area

The following radiation fields have to be monitored in the East Hall:

i) Neutron stray radiation emerging from beam interaction after traversing the shielding structures.

ii) Muons traversing the shielding structures: the only radiological relevant location in the East Hall is downstream of the CHARM beam dump where a dedicated radiation monitor is already installed. The muon fluxes downstream of the T09, T10, and T11 areas are very low; a fact that will be confirmed by dedicated measurements using mobile devices during the commissioning phase after LS2.

iii) Photons from the decay of residual radioactivity in the primary zone.

4.11.3 Radiation monitoring devices

A general description of the CERN radiation monitoring system is given in Ref. [60]. High-pressure hydrogen ionization chambers (20 bar), designated as IG5-H20 AMF, will be used to measure neutrons. Air filled ionization chambers, designated IAM, will be used to measure photons from residual radiation in the primary zone. A ventilation gas monitor, designated as VGM, will monitor the airborne radioactivity released by the ventilation system for the primary zone that guaranties dynamic confinement.

4.11.4 Layout of the future radiation monitoring system

The preliminary layout of the radiation monitoring system related to the East Area Renovation project is shown in Fig. 4-56. The currently installed monitor chambers will be re-used. Therefore, the identifiers of the monitors

to be relocated are also given in Fig. 4-56. This means that only two new, high-pressure hydrogen ionization chambers (indicated as AMF) and one new VGM will need to be installed for the East Area Renovation project.

The layout of the already installed radiation monitoring system related to the IRRAD and CHARM facilities can be found in Ref. [61]. These monitors will remain at their present locations, except PAXEA811N and PAXEA821N. These two monitors will be re-located and their future position is indicated in Fig. 4-56.

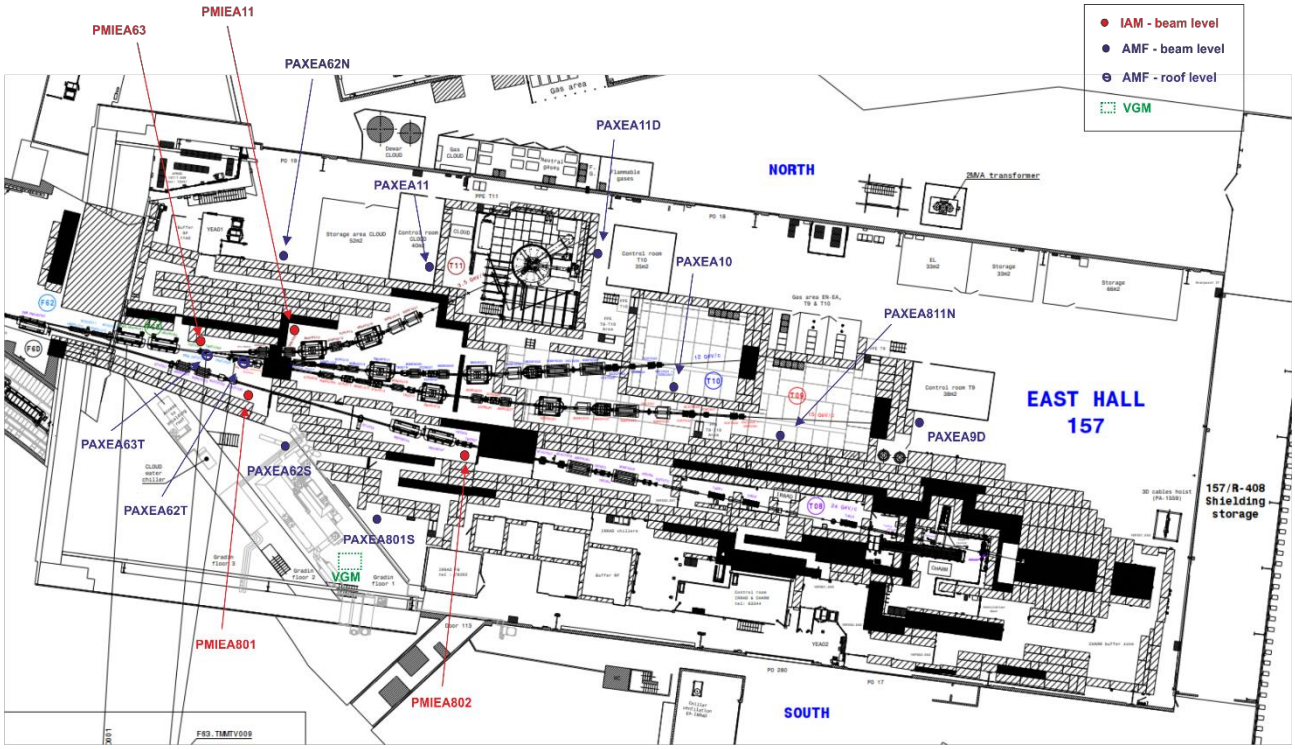

Fig. 4-56: Location and types of radiation monitors (IAM - induced activity monitor, AMF - area mixed field radiation monitor, VGM - ventilation gas monitor) related to the East Area Renovation project. The radiation monitors for IRRAD and CHARM are not indicated [61], except for PAXEA811N and PAXEA821N, that will be relocated.

References

[1] MCB magnet, NORMA database, https://norma-db.web.cern.ch/magdesign/idcard/188/.

[2] M100 L magnet, NORMA database, https://norma-db.web.cern.ch/magdesign/idcard/1903/.

[3] M200 L magnet, NORMA database, https://norma-db.web.cern.ch/magdesign/idcard/1904/.

[4] Specification of the bending magnets for the ISR beam transfer system, ISR/BT group (I-5010-ISR) (CERN, Geneva, November 1967) EDMS 1100428.

[5] M100 magnet, NORMA database, https://norma-db.web.cern.ch/magdesign/idcard/154/.

[6] M200 magnet, NORMA database, https://norma-db.web.cern.ch/magdesign/idcard/160/.

[7] QDS magnet, NORMA database, https://norma-db.web.cern.ch/magdesign/idcard/325/.

[8] QFS magnet, NORMA database, https://norma-db.web.cern.ch/magdesign/idcard/336/.

[9] QFL magnet, NORMA database, https://norma-db.web.cern.ch/magdesign/idcard/335/.

[10] Q100 magnet, NORMA database, https://norma-db.web.cern.ch/magdesign/idcard/334/.

[11] Q200 magnet, NORMA database, https://norma-db.web.cern.ch/magdesign/idcard/350/.

[12] Q100 L magnet, NORMA database, https://norma-db.web.cern.ch/magdesign/idcard/1902/.

[13] Q200 L magnet, NORMA database, https://norma-db.web.cern.ch/magdesign/idcard/1921/.

[14] Q74 L magnet, NORMA database, https://norma-db.web.cern.ch/magdesign/idcard/1281/.

[15] Q120 C magnet, NORMA database, https://norma-db.web.cern.ch/magdesign/idcard/1901/.
[16] Q74 magnet, NORMA database, https://norma-db.web.cern.ch/magdesign/idcard/311/.
[17] Q120 magnet, NORMA database, https://norma-db.web.cern.ch/magdesign/idcard/338/.
[18] MEA19 magnet, NORMA database, https://norma-db.web.cern.ch/magnet/idcard/1343/.
[19] MDX magnet, NORMA database, https://norma-db.web.cern.ch/magdesign/idcard/231/.
[20] CR200 magnet, NORMA database, https://norma-db.web.cern.ch/magdesign/idcard/1906/.
[21] Study of the magnetic coupling between the CR200 and the Q120 C in the new East Area layout, EDMS 2002996 (2018)
[22] MDX L 150 magnet, NORMA database, https://norma-db.web.cern.ch/magdesign/idcard/1905/.
[23] J. Burnet, and K. Papastergiou, Energy Saving; an example of a test facility upgrade with pulsed magnets instead of DC magnets, saving 90% of energy consumption, EDMS 1770483 (2013).
[24] J. Cottet, and J. Burnet, East Area energy balance and possible improvements, EDMS 1255278 (2012).
[25] S. Evrard, East area renovation: notes BE-OP meeting, EDMS 1886001 (2017).
[26] K. Papastergiou, Minutes of meeting with Rende Steerenberg and Lau Gatignon, EDMS 1506818 (2015).
[27] I. Josifovic, and L. Sburlino, Accelerated aging tests of electrolytic capacitors, EDMS 1804172.
[28] L. Sburlino, Lifetime investigation of electrolytic capacitors in power cycling applications, EDMS 1597459 (2016).
[29] E. Coulinge, and K. Papastergiou, Thermal stress and lifetime of power semiconductors in PS transfer lines, EDMS 1458404 (2012).
[30] S. Maestri *et al.,* Study of power converter topologies with energy recovery and grid power flow control Part B: boost converter with energy storage, CERN-ACC-2015-0049, https://cds.cern.ch/record/2016791.
[31] S. Maestri *et al.,* Study of power converter topologies with energy recovery and grid power flow control Part C: a review of alternative structures, CERN-ACC-2017-0089, https://cds.cern.ch/record/2291044.
[32] S. Maestri *et al.,* Study of power converter topologies with energy recovery and grid power flow control. Part A: 2-quadrant converter with energy storage, CERN-ACC-2015-0026, https://cds.cern.ch/record/1994175.
[33] K. Papastergiou, and A. Harle, Electrolytic capacitors failure mechanism, EDMS Folder-0000189820 (2018).
[34] Papastergiou, K., Post-LS2 EIS-chain management specification for power converters, EDMS 2045163 (2018).
[35] K. Papastergiou, Functional specification: Economy mode operation in accelerator transfer lines, EDMS 1493325 (2015).
[36] E. Harrouch, and V. De Jesus, Vacuum control system for the East Area, CERN, EDMS 1737544 (2016).
[37] A. Pilan Zanoni, Description and thermo-mechanical analysis of the beam stoppers BI.STPFA and BI.STPS, EDMS 1698144 (2016).
[38] A. Pilan Zanoni, Thermo-mechanical analysis of the beam stopper BTY.STP103, EDMS 1703654.
[39] A. Pilan Zanoni, Description and thermo-mechanical analysis of the beam stopper BTP.STP10, EDMS 1742948 (2017).
[40] A. Pilan Zanoni, Description and thermo-mechanical analysis of the beam stoppers in the PS extraction (F16, FTA and FTN) lines, EDMS 1691345 (2017).
[41] A. Pilan Zanoni, PS beam stoppers, EDMS 1871447 (2018).
[42] A. Pilan Zanoni, Engineering and design of the new PS beam stoppers, EDMS 1979131 (2018).

[43] A. Pilan Zanoni, Core of the PS beam stoppers, EDMS 1899978 (2018).
[44] V. Agoritsas, Secondary emission chambers for monitoring the CPS ejected beams, Daresbury Symposium on Beam Intensity Measurement, 23–26 April 1968, https://cds.cern.ch/record/299104.
[45] I. Ortega *et al., Jour. Phys.: Conf. Ser.* **763** (2016) 012012, https://doi.org/10.1088/1742-6596/763/1/012012.
[46] E. Harrouch, and M. Lazzaroni, Beam instrumentation needs for the East Area renovation, EDMS 1865542 (2018).
[47] D. Missiaen *et al*., Definition of the MADx output file for survey, EDMS 2052453 (2019).
[48] M. Zerlauth, and R. Mompo, Warm magnet interlock controller software functionality, EDMS 1360775 (2016).
[49] A. Miranda Fontan, and R. Mompo, WIC magnet interlock system for the East Area, EDMS 2037701 (2018).
[50] S. Deghaye, BE-CO plans for LS2, EDMS 1997812 (2018).
[51] S. Evrard, North Area Collimators, EDMS 1505414 (2015).
[52] J. Meignan, Engineering Spec. for the new TCX in the primary Area, EDMS 1889861 (2017).
[53] L. Gentili, TCS collimator plug-in ball support, EDMS 624352 (2016).
[54] M. Lazzaroni, J. Bernhard, and E. Harrouch, Beam stopper, stopper dump and target, EDMS 1786687 (2018).
[55] D. Forkel-Wirth, Zonage radiologique au CERN, EDMS 810149 (2017).
[56] T.T. Böhlen *et al*., *Nuclear Data Sheets* **120** (2014) 211–214, https://doi.org/10.1016/j.nds.2014.07.049.
[57] A. Ferrari *et al.,* FLUKA: a multi-particle transport code, CERN (2005), CERN-2005-10, INFN/TC_05/11, SLAC-R-773, http://dx.doi.org/10.5170/CERN-2005-010.
[58] E. Iliopoulou, and R. Froeschl, Radiation Protection assessment of the shielding design of the East Area target zone and test beamlines, EDMS 2058239 (2018).
[59] E. Iliopoulou, and R. Froeschl, Status update on the RP assessment for the East Area Renovation Project, EDMS 1974733 (2018).
[60] D. Perrin, Description of the CERN radiation and environmental monitoring system, CERN-RP-2017-027-REPORTS-TN, EDMS 1723230 (2017).
[61] R. Froeschl, Radiation protection assessment of the proton irradiation and the CHARM facility in the East Area, CERN-RP-2014-008-REPORTS-TN, EDMS 1355933 (2014).